

# Search for a Heavy Resonance Decaying into Tau Leptons

Andrew Ausherman

Department of Physics, University of Colorado at Boulder  
Defended November 5, 2015

## Abstract

This thesis reports a search for identifying the theoretical  $Z'$  boson at the LHC. It was assumed that the  $Z'$  is created at rest, and an algorithm exploiting the geometry of the decay was developed to reconstruct the mass of the  $Z'$ . In testing, it was discovered that the  $Z'$  is boosted in simulations, invalidating the proposed algorithm. The new approach to mass reconstruction involved looking for correlations between properties of the taus and their decay products. No successful algorithm that reconstructed the generated mass of the  $Z'$  was found. However, analysis revealed that the difference in  $P_T$ , denoted  $\Delta P_T$ , of the electron and muon was equivalent to the missing transverse energy in  $Z'$  decays, but this was not always the case in background signals. This suggests that  $\Delta P_T$  can provide a means of further separating  $Z'$  decays from similar processes.

*Thesis Advisor:*

John Cumalat - Physics

*Thesis Committee:*

John Cumalat – Dept. of Physics  
James Thompson – Dept. of Physics  
Paul Strom – Honors Program

## Key Terms

CERN: The European Organization for Nuclear Research is home to some of the largest and most complex scientific instruments in the world. Thousands of CERN affiliates work to answer questions about the fundamental nature of the universe.

LHC: The Large Hadron Collider is the largest particle accelerator in operation. It collides Protons in a 27 km tunnel deep underground at immense energies.

CMS: The Compact Muon Solenoid experiment is a large, general-purpose detector on the LHC. Data collected from collisions inside the detector are used to probe a wide range of physics.

Beam Spot: This is the region inside the detector filled with proton collisions, typically accurate to 100  $\mu\text{m}$  in x and y, and to a few centimeters in z.

Primary Vertex: The actual point where particles collide, found by reconstructing tracks of the debris and performing a 3D fit to find an interaction point.

Transverse Plane: Same as the xy-plane in Cartesian coordinates. Inside the detector, it is the plane perpendicular to the beam tunnel.

Transverse Momentum:  $P_T = \sqrt{P_x^2 + P_y^2}$

Electron Volt (eV): A unit of energy equivalent to the work needed to accelerate an electron through a potential difference of 1 Volt. More specifically,  $1 \text{ eV} = 1.602 \times 10^{-19} \text{ Joules}$ . In this project, most values are presented in gigaelectronvolts (GeV), which is equal to  $10^9 \text{ eV}$ . In High Energy Physics, and in this project, the units of momentum are  $[\text{GeV}/c]$  and the units of mass are  $[\text{GeV}/c^2]$ , where  $c$  is the speed of light ( $c = 3.0 \times 10^8 \text{ m/s}$ ). This is the convention used in all calculations, and actually dividing by  $c$  is unnecessary.

## List of Figures

Figure 2.1 Standard Model of Particle Physics	3
Figure 2.2 Diagram for a tau decay	9
Figure 2.3 Perspective view of the CMS detector	12
Figure 2.4 Cross-section of the CMS detector	12
Figure 2.5 Diagrams for $W^+W^-$ and $t\bar{t}$	15
Figure 4.1 A Picture of the $Z'$ decay	19
Figure 4.2 X and Z distances from the primary vertex to the line connecting the tau decay vertices	23
Figure 4.3 A visual representation of one event	24
Figure 4.4 Combined momentum of the taus	25
Figure 4.5 Drell-Yan diagram	26
Figure 4.6 Initial fits for $P_T$ and $P_Z$	29
Figure 4.7 A plot comparing the total momenta of the electron and muon	30
Figure 4.8 The calculated mass of the $Z'$ across all events.	31
Figure 4.9 Comparisons of combined $P_Z$ for the taus and their daughters, and tau energy comparison	32
Figure 4.10 Comparing energy of taus with their daughter particles	33
Figure 4.11 Estimated mass of $Z'$ using the fits for $P_Z$	34
Figure 4.12 3D fit of tau $P_T$	35
Figure 4.13 Comparison of the values of $P_T$ for each tau, and the combined $P_T$ of the taus	35
Figure 4.14 Estimated mass of $Z'$ using fit for $P_T$	37
Figure 4.15 Calculated transverse mass of the $Z'$	38
Figure 4.16 Comparing $P_T$ for the electron and muon, and the angle between their $P_T$ vectors	39
Figure 4.17 A momentum vector broken into components	40
Figure 4.18 Ratio of transverse to total momentum for the taus and their daughter particles	41
Figure 4.19 Ratio of the Z to the total momentum for the taus and their daughter particles	41
Figure 4.20 Diagram of boosted tau decay	42
Figure 4.21 Comparison of the total momenta of the taus to their daughter particles	43
Figure 4.22 Ratio of the taus' momenta, and the momenta plotted against each other	44
Figure 4.23 Mass of the electron and muon, calculated with and without missing energy	45
Figure 4.24 Comparison of the missing energy and $\Delta P_T$ for $Z'$ and $W^+W^-$ decays	47
Figure 4.25 Comparison of the missing energy and $\Delta P_T$ for $t\bar{t}$ decays	48
Figure 5.1 $Z'$ mass calculated using fits for $P_Z$ and $P_T$	49
Figure 5.2 Mass of the electron and muon, using missing energy	50
Figure 5.3 Generated mass of the $Z'$	50

## TABLE OF CONTENTS

1. Introduction .....	1
2. Background.....	3
2.1. The Standard Model .....	3
2.2. Particle Interactions.....	6
2.3. Invariant Mass Calculation .....	7
2.4. Branching Fractions of the Tau .....	9
2.5. CMS Detector .....	12
2.6. Types of Data.....	14
2.7. Selection Cuts.....	15
3. Methods.....	18
4. Procedure .....	20
4.1. Geometric Approach .....	20
4.2. Early Fits For $P_z$ and $P_T$ .....	27
4.3. Comparison of Trajectory Directions .....	39
4.4. Missing Energy .....	45
5. Results.....	49
6. Discussion .....	51
7. Conclusion.....	54
8. References.....	56
9. Appendix.....	57
A.1. $P_z$ Mass.....	57
A.2. Comparing the mass of $e + \mu$ to various quantities .....	58

## 1. Introduction

With the second run of the LHC underway, and at record-breaking energy, we are able to investigate the nature of elementary particles like never before. With such high-energy collisions, heavier theoretical particles, including the infamous Higgs, can be created inside the accelerator. One such particle is the  $Z'$  boson. This is theorized to be another version of the  $Z$  boson, with similar couplings, described by the Standard Model. It has various implications for theories on physics beyond the Standard Model, which depend on its mass [1,2]. Confirmation of the existence of the  $Z'$ , and measurement of its mass, would lead to a greater understanding of Elementary Particle Physics.

In this project, we investigate the di-tau decay channel of the  $Z'$  with the intent of accurately reconstructing its mass. This decay channel, producing one tau and one anti-tau, is not unique to the  $Z'$ . It is observed in decays of other particles, including the Higgs [3,4]. Therefore, CMS collaborators have already developed tau analysis software adequate for this project [5]. Additionally, the tau decay channels chosen are the electron-muon channels. These processes are very clean to identify, but they also produce neutrinos, which escape the CMS detectors, carrying away energy in the process [6,7].

The missing energy carried off by the neutrinos complicates the  $Z'$  mass reconstruction. Only the electron and muon are detected, and they only account for a third of the total decay products. This means that the visible mass of the decay products is far below the generated mass of the  $Z'$  in simulations, so a new technique for reconstructing the  $Z'$  mass is needed for raw data.

If an algorithm reconstructing the mass of the system containing the taus is found, it could have implications for future experiments. Many heavier particles decay into taus, and being able to reconstruct the mass of these particles at a range of energies would aid in studying their properties. Additionally, more work has been done to study the hadronic decay channel of taus [7,8], so studying the electron/muon channels adds to our understanding of tau decays in general.

## 2. Background

### 2.1 The Standard Model

THE STANDARD MODEL					
	Fermions			Bosons	
Quarks	$u$ up	$c$ charm	$t$ top	$\gamma$ photon	Force carriers
	$d$ down	$s$ strange	$b$ bottom	$Z$ Z boson	
Leptons	$\nu_e$ electron neutrino	$\nu_\mu$ muon neutrino	$\nu_\tau$ tau neutrino	$W$ W boson	
	$e$ electron	$\mu$ muon	$\tau$ tau	$g$ gluon	

**Figure 2.1** The Standard Model of particle physics, which describes elementary particles and their interactions [9].

The Standard Model hypothesizes that matter is composed of three kinds of elementary particles: quarks, leptons and mediators. Quarks and leptons are all fermions, or particles with half integer spin, while the mediators are bosons, or particles with integer spin. The quarks and leptons in Fig. 2.1 fall into three generations, with the first column representing the first generation, the second column representing the second generation, and the third column the third. Each generation of matter is heavier than the one before it, so just as the electron is lighter than the muon or the tau, the up and down quarks are lighter than their quark cousins. There are six ‘flavors’ of quarks, shown in Fig. 2.1. In addition, each quark comes in three ‘colors’, where color is a property governing strong interactions analogous to electric charge governing electromagnetic interactions. It

is important to note that individual quarks are never observed; they always come in bound, colorless states called hadrons. Baryons are hadrons with three quarks, such as the proton and neutron; all three colors of quark are found in these particles, making them 'colorless'. Mesons are hadrons with a quark-antiquark pair, such as the pion; the color of each quark must be the same for these particles in order to be colorless. Similarly there are six 'flavors' of leptons, of which the most recognizable is the electron. Finally, there are mediators for each elementary interaction- the photon for electromagnetic forces, two charged Ws and a neutral Z for the weak force, and the gluon for the strong force that mediates quark interactions [10].

Paul Dirac, a pioneer of elementary particle physics, developed the wave equation that bears his name in 1927 to describe free electrons with relativistic energy. There was a problem with this description as the equation implied that there are two solutions to problems involving electron scattering: one in a positive energy state and one in a negative energy state. Ernst Stueckelberg and Richard Feynman gave an explanation for this in the 1940s that has since been proven true. They suggest that the negative-energy solutions to Dirac's equation are actually positive-energy states of different particles. This interpretation was supported at the time by the discovery of the positron. This particle has all the same properties as the electron, except that it is positively charged. Similarly, all particles described by the Standard Model have twins with opposite charge, called antiparticles.

Antimatter requires sophisticated facilities such as the ones at CERN for its production. It takes a lot to isolate antiparticles from controlled interactions, and storing them is a problem because matter and antimatter annihilate when they are



brought into contact. There is also no explanation yet for why the universe seems to have more matter than antimatter [10].

Around the same time as the discovery of the positron, it was discovered that in instances of beta decay, where a radioactive nucleus decays into a lighter one with the emission of an electron, the energy of the outgoing electron was less than what conservation of energy would imply. Wolfgang Pauli proposed that another particle is emitted with the electron and makes up the difference in energy. This particle had to be electrically neutral and light in mass, so it was called the neutrino, or 'little neutral one'. Neutrinos turned out to be very difficult to detect, and their existence was not confirmed until the 1950s. They do not leave a track, and decay into no other particles. They interact so weakly with other matter that neutrinos regularly pass through the earth with no interaction. Neutrinos are classified as leptons, and there is one for each generation of matter: an electron neutrino, a muon neutrino and a tau neutrino. In addition there are three antineutrinos, one for each neutrino. In interactions in the LHC, neutrinos regularly escape detectors, and their existence is established only by looking for missing energy [10].

The Standard Model has been verified by many experiments, but it is not a complete theory. It does not account for the force of gravity, the weakest of the four fundamental forces, as well as other phenomena such as dark matter. It describes 61 'elementary' particles (including antiparticles and different colored quarks/gluons), which some argue are too many for a fundamental theory, and there are over 20 arbitrary parameters needed in the Standard Model, which would have to be

explained by a ‘final’ theory. There are many theories for beyond Standard Model physics, but none are yet supported by direct experimental evidence [10].

## *2.2 Particle Interactions*

There are four fundamental forces that govern particle interactions. The strongest is called the “strong force”, responsible for holding the nuclei of atoms together. The next strongest is the electromagnetic force, which binds electrons to atoms. Then comes the weak force, which governs radioactive decay. The weakest force is gravity, which has not been seen to play a role in elementary particle physics. Each force is mediated by the exchange of a particle and has its own physical theory that describes how it works. In particle physics, interactions are described by Feynman diagrams, which show how processes evolve in both time and position. In addition to the established conservation of energy and momentum, elementary particle interactions introduce new conservation laws [10].

All interactions conserve electric charge and color. These quantities are conserved at each vertex in the Feynman diagram, and thus for the diagram as a whole. In addition, baryon number and lepton number must be conserved at vertices. Baryon number is defined as the number of baryons minus the number of antibaryons. Similarly, lepton number is defined as the number of leptons minus the number of antileptons. In most cases, including the decays in this project, there is no cross-generation mixing of leptons, so electron number, muon number, and tau number are independently conserved (note: neutrinos have the same lepton number as the other lepton in their generation). The last important conservation is

for quark flavor, but here flavors are only approximately conserved. They are conserved at strong and electromagnetic vertices, but not weak ones [10].

There is typically more than one Feynman diagram that can describe an interaction. Each diagram has a scattering amplitude associated with it, which contains the dynamic information of the interaction. This is calculated using the appropriate Feynman rules that impose conservation laws at each vertex. This amplitude can then be used to calculate decay rates and cross sections of interactions. Each Feynman diagram has its own scattering amplitude, and the total for a specific interaction is just the sum of individual amplitudes. This process is used to calculate rates and cross sections for decays and collisions, which is essential information for designing an experiment [10].

### *2.3 Invariant Mass Calculation*

In this project, the mass of a particle must be calculated from its decay products. This process is not as simple as adding the masses of the daughter particles. In relativistic kinematics, the notation of the energy-momentum four-vector is introduced. This resembles the position-time four-vector used to perform Lorentz transformations. This four-vector,  $p_\mu$ , is defined as follows:

$$p_\mu = (E/c, P_x, P_y, P_z) \text{ (Contravariant Form),}$$

$$p^\mu = \begin{pmatrix} E/c \\ -P_x \\ -P_y \\ -P_z \end{pmatrix} \text{ (Covariant Form),}$$

$$\text{where } E = \sqrt{m^2 c^4 + P^2 c^2}$$

We need both the contravariant and covariant forms in order to calculate the invariant mass:

$$M = \sqrt{p_\mu p^\mu} = \sqrt{\frac{E^2}{c^2} - \vec{P}^2}$$

$$\text{with } \vec{P}^2 = P_x^2 + P_y^2 + P_z^2$$

This formula is invariant, so it yields the same value in every reference frame. In the context of this project, we have one parent particle that decays into two daughter particles. There is always a reference frame in which a single particle is at rest, i.e.  $\vec{P} = 0$ , so the invariant mass of the parent particle is equal to its rest mass. Since energy and momentum are conserved in the decay, the invariant mass of the system containing both daughter particles will be equal to this rest mass as well. To calculate this, we need the mass and momentum for each daughter particle. In the case of two decay products, this can be expressed as two energy-momentum four-vectors:

$$p_\mu^{(1)} = \left( E^{(1)}/c, P_x^{(1)}, P_y^{(1)}, P_z^{(1)} \right) \quad p_\mu^{(2)} = \left( E^{(2)}/c, P_x^{(2)}, P_y^{(2)}, P_z^{(2)} \right)$$

Then the energy-momentum four-vector of the system containing both particles is just the summation of the individual four-vectors:

$$\begin{aligned} P_\mu &= \left( \frac{E^{(1)} + E^{(2)}}{c}, P_x^{(1)} + P_x^{(2)}, P_y^{(1)} + P_y^{(2)}, P_z^{(1)} + P_z^{(2)} \right) \\ &= \left( \frac{E^{(1)} + E^{(2)}}{c}, \vec{P}^{(1)} + \vec{P}^{(2)} \right) \end{aligned}$$

Now we can compute the invariant mass:

$$M = \sqrt{P_\mu P^\mu} = \sqrt{\left(\frac{E^{(1)} + E^{(2)}}{c}\right)^2 - (\vec{P}^{(1)} + \vec{P}^{(2)})^2}$$

$$\text{where } (\vec{P}^{(1)} + \vec{P}^{(2)})^2 = \sqrt{(\vec{P}^{(1)} + \vec{P}^{(2)}) \cdot (\vec{P}^{(1)} + \vec{P}^{(2)})}$$

#### 2.4 Branching Fractions of the tau

Particles in the Standard Model typically decay to a variety of final states. Any valid Feynman Diagram that can be drawn for a specific decay has a probability of occurring. The decay channels, also known as decay modes or basis modes, of a particle represent the different final states. The branching fraction of any given decay channel is the probability of seeing that particular decay. The principal decay of interest in this project is that of the tau particle. Taus have 31 recognized decay channels, i.e. channels with a non-negligible branching fraction. See Table 2.1 for a list of all the tau decay modes. The two modes investigated in this project are  $\tau \rightarrow e^- \bar{\nu}_e \nu_\tau$  and  $\tau \rightarrow \mu^- \bar{\nu}_\mu \nu_\tau$  with branching fractions of  $17.83 \pm 0.04 \%$  and  $17.41 \pm 0.04 \%$  respectively [6]. Fig. 2.2 shows a Feynman diagram for this process.

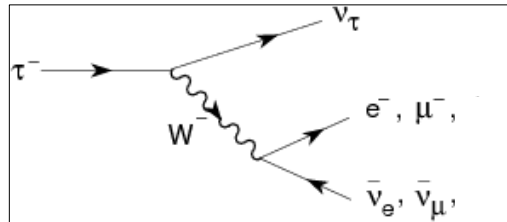


**Figure 2.2** Diagram for a tau decay resulting in an electron or muon. In this diagram, the horizontal axis represents time, and the vertical axis represents position. The  $W^-$  mediator exists on an internal line, and is a virtual particle; it decays very quickly, and thus cannot be detected [11].

Table 2.1 Decay modes and fit values (%) for 2012 tau data [3]

$e^- \bar{\nu}_e \nu_\tau$	$17.83 \pm 0.04$
$\mu^- \bar{\nu}_\mu \nu_\tau$	$17.41 \pm 0.04$
$\pi^- \nu_\tau$	$10.83 \pm 0.06$
$\pi^- \pi^0 \nu_\tau$	$25.52 \pm 0.09$
$\pi^- 2\pi^0 \nu_\tau$ (ex. $K^0$ )	$9.30 \pm 0.11$
$\pi^- 3\pi^0 \nu_\tau$ (ex. $K^0$ )	$1.05 \pm 0.07$
$h^- 4\pi^0 \nu_\tau$ (ex. $K^0, \eta$ )	$0.11 \pm 0.04$
$K^- \nu_\tau$	$0.700 \pm 0.010$
$K^- \pi^0 \nu_\tau$	$0.429 \pm 0.015$
$K^- 2\pi^0 \nu_\tau$ (ex. $K^0$ )	$0.065 \pm 0.023$
$K^- 3\pi^0 \nu_\tau$ (ex. $K^0, \eta$ )	$0.048 \pm 0.022$
$\pi^- \bar{K}^0 \nu_\tau$	$0.84 \pm 0.04$
$\pi^- \bar{K}^0 \pi^0 \nu_\tau$	$0.40 \pm 0.04$
$\pi^- K_S^0 K_S^0 \nu_\tau$	$0.024 \pm 0.005$
$\pi^- K_S^0 K_L^0 \nu_\tau$	$0.12 \pm 0.04$
$K^- K^0 \nu_\tau$	$0.159 \pm 0.016$
$K^- K^0 \pi^0 \nu_\tau$	$0.159 \pm 0.020$
$\pi^- \pi^+ \pi^- \nu_\tau$ (ex. $K^0, \omega$ )	$8.99 \pm 0.06$
$\pi^- \pi^+ \pi^- \pi^0 \nu_\tau$ (ex. $K^0, \omega$ )	$2.70 \pm 0.08$
$K^- \pi^+ \pi^- \nu_\tau$ (ex. $K^0$ )	$0.294 \pm 0.015$
$K^- \pi^+ \pi^- \pi^0 \nu_\tau$ (ex. $K^0, \eta$ )	$0.078 \pm 0.012$
$K^- K^+ \pi^- \nu_\tau$	$0.144 \pm 0.005$
$K^- K^+ \pi^- \pi^0 \nu_\tau$	$0.0061 \pm 0.0025$
$h^- h^- h^+ 2\pi^0 \nu_\tau$ (ex. $K^0, \omega, \eta$ )	$0.10 \pm 0.04$
$h^- h^- h^+ 3\pi^0 \nu_\tau$	$0.023 \pm 0.006$
$3h^- 2h^+ \nu_\tau$ (ex. $K^0$ )	$0.0839 \pm 0.0035$
$3h^- 2h^+ \pi^0 \nu_\tau$ (ex. $K^0$ )	$0.0178 \pm 0.0027$
$h^- \omega \nu_\tau$	$2.00 \pm 0.08$
$h^- \omega \pi^0 \nu_\tau$	$0.41 \pm 0.04$
$\eta \pi^- \pi^0 \nu_\tau$	$0.139 \pm 0.010$
$\eta K^- \nu_\tau$	$0.0152 \pm 0.0008$

The rest of the tau decay channels are hadronic and produce what are called jets [6]. A jet is a cone of hadrons that is produced in a collision. Since individual quarks or gluons cannot exist in confinement, when they scatter, it takes less energy to create new quarks than it does to separate quarks. The result is a flurry of hadrons all traveling in roughly the same direction as the original quark.

Among other reasons, the hadronic decay channels of the tau have been studied for the insight they give to jets. Jet reconstruction is an important tool for analyzing many of the interactions inside the LHC. However, there are many hadronic decay modes associated with the tau, which can produce varying numbers of jets. This makes for a complicated system that can be difficult to model [7,8]. The electron/muon decay channels, which account for about a third of individual tau decays, are simpler to isolate within data and do not produce jets, so they are chosen as the primary channel of investigation for this project.

### *2.5 CMS Detector*

The CMS detector is installed at the LHC roughly 100 meters underground near the French village of Cessy. The LHC is housed in a 27 km tunnel on the border of France and Switzerland. It is designed to provide a luminosity of  $10^{34} \text{ cm}^{-2}\text{s}^{-1}$  through collision of two proton beams at 7 TeV each [12].

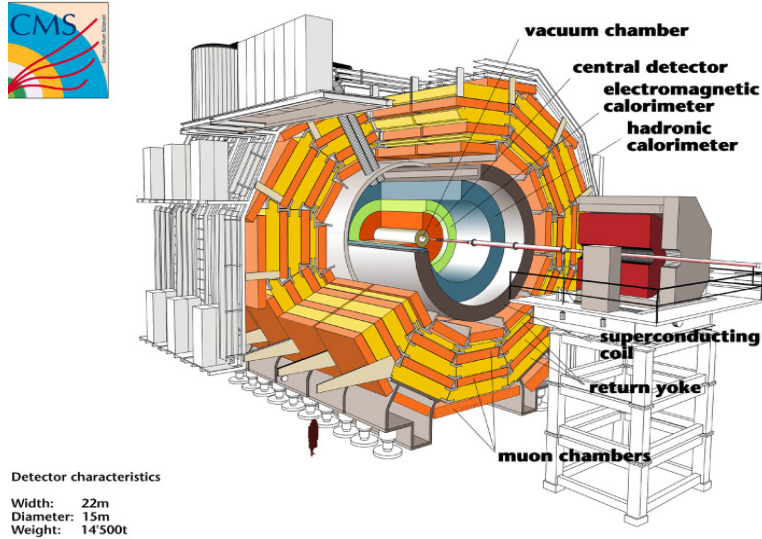


Figure 2.3 Perspective view of the CMS detector, situated underground on the LHC [13].

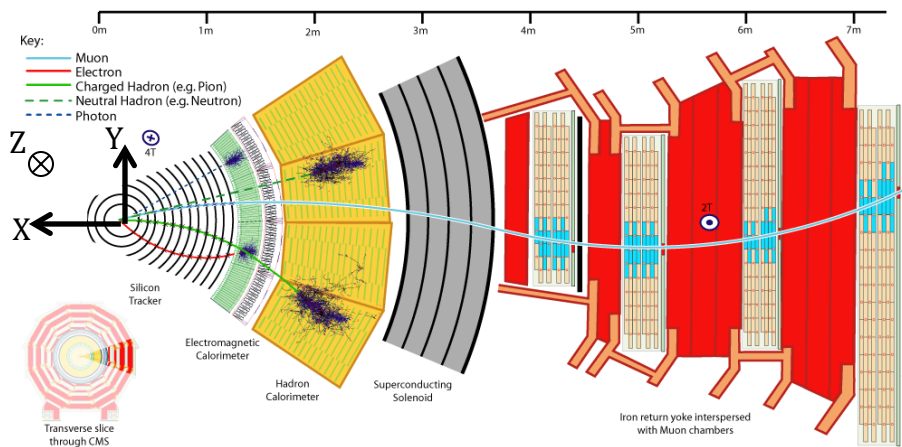


Figure 2.4 Cross-section of the CMS detector, with coordinate axes defined [13].

The superconducting solenoid used by CMS is the largest in the world at 13 m long and 6 m in diameter, and provides a 4 T magnetic field. This gives sufficient bending power to curve the tracks of fast charged particles. The innermost layer of the detector is the silicon tracker, which tracks the path of charged particles through the detector. By measuring how much a particle's track bends, its momentum can be determined. The next layer is the electromagnetic calorimeter, made of lead



tungstate, which detects and measures the energy of particles such as electrons and photons. After that the hadron calorimeter, consisting of brass interspersed with plastic scintillators, registers hadrons that enter the detector and measures their energy. Past the superconducting solenoid is the iron return yoke, which has multiple layers of drift tubes, cathode strip chambers and resistive plate chambers, designed to identify and measure the energy of muons. For a complete description of the CMS detector, see [12].

## *2.6 Data*

Huge amounts of data are collected in the LHC while it is running. Since only a fraction of this contains physics of interest, there are many steps designed to reduce the amount of data going out without losing interesting events. Inside the detector, hardware and software is used to skim the data as it is being created, in a process called ‘triggering’. The raw data produced in this process are sorted into primary datasets at CERN, and then passed to one (or more) of seven central (Tier-1) computing centers around the world. These centers skim the data to reduce its size and eliminate unnecessary events. They also produce most of the reconstructed (RECO) data and Analysis Object Data (AOD). RECO data reconstructs the events inside the detector, including all the physics objects. AOD distills this data into a smaller package containing the information needed by physicists. The data are then passed to smaller (Tier-2) data centers, where research groups apply their own selection criteria. This is the level where actual analysis occurs [14].

The other type of data used in this project comes from Monte Carlo simulations. These simulations are executed in a CERN program designed to accurately model the motion of particles through matter [15]. This software can be used to create a virtual set of events modeling a wide range of physical situations. These data are then passed through additional software that mimics the detector, reconstructing the events in the same way raw data will be handled. Simulated data are helpful for many tasks, including searches for new particles. Since no real-world data for these particles exist, simulations can be used to predict their behavior based on the physical theory and the mechanics of similar particles. In this project, the process of  $Z'$  creation is modeled virtually, and analysis is performed on this data [14,15].

### *2.7 Background Signals and Selection Cuts*

There are many physical processes that produce decay products similar to those produced in the  $Z'$  decay. Two notable examples include  $W^+W^-$  and  $t\bar{t}$ . The taus we are investigating actually decay into  $W$  bosons (along with a tau neutrino to preserve lepton number) so they are difficult to distinguish from  $W^+W^-$ , pictured on the left in Fig. 2.5. The only difference between these events is that the  $Z'$  decay produces two extra neutrinos, which are never detected. Similarly, top quarks decay into  $W$  bosons, and produce an electron, muon, and two neutrinos. However,  $t\bar{t}$  events also produce jets, as shown in the diagram on the right of Fig. 2.5.

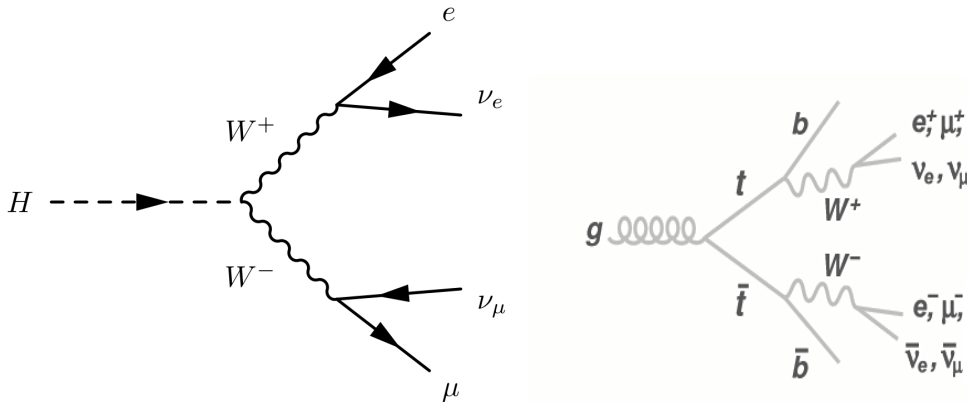


**Figure 2.5** The Feynman diagram on the left shows a Higgs boson decaying into  $W^+W^-$ . This results in an electron, muon and two neutrinos; just like the  $Z' \rightarrow \tau^+\tau^-$  decay we investigate, only the electron and muon are seen. The Feynman diagram on the right shows a gluon decaying into  $t\bar{t}$ . This produces the same products as the  $W^+W^-$  decay, but also produces two b-jets. [16], [17]

Once an algorithm capable of reconstructing the mass of the  $Z'$  is found, it must be tested against these background processes. We only want to determine the mass for events that actually involve a  $Z'$  decay, so steps must be taken to separate out the background signals. Initially this is done through selection cuts.

Before my involvement in this project, some selection cuts were applied to the simulated data to reduce events originating from  $W^+W^-$ ,  $t\bar{t}$ , and other backgrounds. Some of the cuts ensure that there is a pair of taus that decay finally into an electron and muon, and in the case where there are multiple such pairs, the one with the highest scalar sum of transverse momentum is chosen. The electron and muon are required to have opposite charges, since the original  $Z'$  is electrically neutral, and their trajectories must be roughly antiparallel, due to restriction in their decay direction caused by the large mass of the parent particle. The transverse momenta of the electron and muon are required to be above 20 GeV/c, so as to separate signals with energy too low to be coming from our generated  $Z'$ . The missing energy, representing the energy carried away by neutrinos, must also

exceed 20 GeV/c. Additional cuts separate out events with jets, which helps reduce the background signals discussed above [4]. After this, most events do represent the decay we are investigating.

Two additional cuts were applied during this project to further reduce the number of events. The first restricted the combined mass of the taus so that events with masses below 1400 GeV/c<sup>2</sup> or above 1600 GeV/c<sup>2</sup> were discarded. Since the Z' is generated at 1500 GeV/c<sup>2</sup> in simulations, events that differ by this value by more than 100 GeV/c<sup>2</sup> cannot represent the decays we are looking for. The 100 GeV/c<sup>2</sup> is used as a buffer for systematic errors in the reconstruction process [4]. The second cut restricted the angle between the transverse momentum vectors of the electron and muon to be between 3 radians and  $\pi$  radians. The events that this cut eliminates show a wide range of angle values and are unlikely to represent the Z' decay we are investigating. After these cuts were applied, many plots were remade to see if there was any noticeable change. The smaller number of events was not seen to change the appearance or statistics of any of these plots, due to the high number of total events. For this reason, plots from before and after the cuts are included in this thesis.

### 3. Methods

To generate  $Z'$  bosons at 1500 GeV in a simulation, code was written that specifies the conditions of the events. It was developed prior to my involvement in the project, and any changes made to it during the project were made by another project member. Running the code simulates thousands of processes containing the  $Z' \rightarrow \tau^+\tau^-$  decay we are investigating. The output of the software that performs this task is a dataset containing the information produced in the Monte Carlo simulations. Since these are generated events, information on the momentum, decay vertex, and charge of the tau particles is written to the file. All the same information is provided for the electrons and muons. Additionally, the generated and reconstructed beam spot positions are included for each event. After this, the data are put through the selection cuts described in section 2.7.

At this point, there are approximately 1400 events left, constituting the data that will be used to develop and test our algorithm. To work with the data, I wrote a program in C++. This program reads in the data associated with each event to a new object class designed for this project. This class stores all the data associated with an event and contains functions that can perform a number of quick calculations on the data, such as finding the mass of the system, calculating the distances particles travel before decaying, and applying additional cuts.

Analysis was done on this data throughout the project, mainly by creating histograms. To do this, code is added to the program to calculate a certain quantity, such as the energy of a tau, for each event and write the values to a text file. This text file is then imported to the CMS software framework, where the ROOT analysis

software, which is used by a majority of CMS collaborators for data analysis, is used to fill a histogram with the values in the text file. 1D, 2D and 3D histograms can be made by this method, but a majority of histograms produced for this project were 1D or 2D [14].

Some basic analysis can be done directly in ROOT, such as calculating the mean and RMS values. The rest of the analysis was done outside of ROOT. Fits were approximated using Mathematica. Error calculation was done primarily in the program used to analyze the generated data. In all of these cases, resources were consulted to ensure that calculations were performed correctly. ROOT, in particular, has many help files that were used to customize the histograms created [14].

## 4. Procedure

### 4.1 Geometric Approach

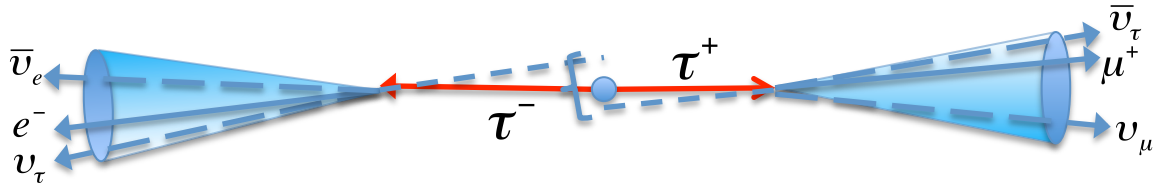


**Figure 4.1** A picture of the  $Z'$  decay. The blue dot represents the primary vertex, where the  $Z'$  was created before decaying into the taus. The taus then decay into an electron, a muon, and 4 neutrinos. Only the electron and muon are detected.

Our first approach to solving this problem is a geometric one. Fig. 4.1 shows the decay of the  $Z'$  into two tau leptons, traveling back-to-back. The negatively charged tau decays into an electron and two neutrinos. The positively charged anti-tau decays into a positively charged anti-muon and two additional neutrinos. The final products that are observed in the detectors are the electron and the anti-muon. Another version of this process will involve the positively charged tau decaying into a positron, with the other tau decaying into an ordinary muon. The results are essentially the same: a lepton and an anti-lepton are observed in the detectors. With this information, we look for a way to find the mass of the taus.

One notable feature of Fig. 4.1 is that the slopes of the lines representing the individual tau decays are equal. Thus if we can draw lines from the primary vertex to individual points on the trajectories of the electron and muon, we can make direct comparisons of their slopes. This is the basis for the proposed algorithm. The equation that must be satisfied is:

$$\frac{e_z - z_0}{\sqrt{(e_x - x_0)^2 + (e_y - y_0)^2}} = \frac{z_0 - \mu_z}{\sqrt{(x_0 - \mu_x)^2 + (y_0 - \mu_y)^2}}$$

where  $(e_x, e_y, e_z) = \text{points on the electron's path}$

$(\mu_x, \mu_y, \mu_z) = \text{points on the muon's path}$

$(x_0, y_0, z_0) = \text{primary vertex for event}$

Here the  $(e_z - z_0)$  term represents the rise of the slope and the term in the denominator is the run. The primary vertex is the reconstructed interaction point that trajectories are traced back to. Points on the electron and muon paths are given by the equation of the line that describes them, which is determined geometrically. This formula essentially draws a line between the primary vertex and every point on the electron's trajectory, and then calculates the slope of these lines. It then does the same for the muon's trajectory and compares the slopes. If the slopes are equal, then the lines described by these slopes must represent the path of the tau particles, which decay back-to-back to conserve momentum. From here the distance that the individual tau particles travel before decaying can be calculated, which can be used to estimate the combined energy of the taus.

One potential problem of this algorithm is the possibility of multiple lines having the same slope. In Fig. 4.1 it is clear that any point can be chosen on the decay paths of the electron or muon and a line can be drawn through the primary vertex such that it intercepts the other lepton's trajectory. It is important to note, however, that this diagram shows the process in two dimensions. The trajectories of the leptons also have a component in the z direction, which goes into the page in the diagram. Now there will be at least one point on each trajectory such that a line can be drawn between them that will go through the primary vertex. However, there is nothing strictly preventing other such points to exist; they are just very unlikely. For instance, if neither tau particle acquires any momentum in the z direction, then their



decay will be represented in the two dimensional figure, and the algorithm will not work. We look at enough data points that we can safely ignore these rare occurrences.

Before the algorithm was implemented into software that can process large numbers of events, it was tested on one individual simulated event. The coordinates of the primary vertex, the point where the electron was detected, and the point where the muon was detected were used along with the components of the electron and muon momenta to test the algorithm. Working through the algorithm by hand, no solution was found. It did not appear that there was a line through the primary vertex that could connect the trajectories of the electron and muon. The algebra was re-checked a few times and no error was found. The algorithm was tested on another data point and was found again to be ineffective.

To investigate this matter further, we looked at all the events and drew a line connecting the points where the individual tau particles decay. Then, the distance from the generated primary vertex to the closest point on this line was calculated for each event. Since the primary vertex is thought to lie on this line, this distance should be zero for almost all events. This was done by finding a formula for the distance between the primary vertex and any point on the line connecting the tau vertices, and minimizing it according to the following formula:

$$\frac{d}{dt} \left( \sqrt{(x_1 - x' + (x_2 - x_1)t)^2 + (y_1 - y' + (y_2 - y_1)t)^2 + (z_1 - z' + (z_2 - z_1)t)^2} \right) = 0$$

where  $(x_1, y_1, z_1)$  and  $(x_2, y_2, z_2)$  are the vertices where the taus decay  
and  $(x', y', z')$  is the primary vertex

Someone with a background in Calculus might wonder if this formula is actually maximizing this distance instead. However, the maximum distance has no solution because the equation describing the line connecting the tau vertices extends indefinitely, making the maximum distance infinite. Therefore the equation has only one solution: the minimum distance. This distance should equal zero for every event because the taus start at the primary vertex and travel a distance before decaying. However, the average distance between the primary vertex and this line was found to be 0.828016 cm. There were no events for which the distance was zero. This meant one of two things. Either the code used to test these distances was not working properly or the initial picture of the decay, shown in Fig. 4.1, was wrong.

The code was tested in several ways. First, a third-party tool was found online that calculates the minimum distance between a point and a line, and was used to confirm the results of the code used in this project. It produced the same distances for a number of events. Secondly, distances for a few events were calculated manually, and still no discrepancy was found. Finally, simple points and lines were created and the distance formula was confirmed to work on these. For instance, a line with a slope of 1 was created to go through the origin and the program calculated the distance from the origin to this line to be zero. The distance was also calculated from easy points, such as (1,0,0), (0,1,0) and (0,0,1). Each time, the distance was correctly calculated.

At this point, all members on the project agreed that there was a problem with an initial assumption of the project. The tau leptons were not decaying back-to-

back as originally thought. The x, y and z components of the distance from the primary vertex to the line connecting the tau vertices were computed for each event and histograms were created displaying the trends. The x and z components of the distances are shown in Fig. 4.2:

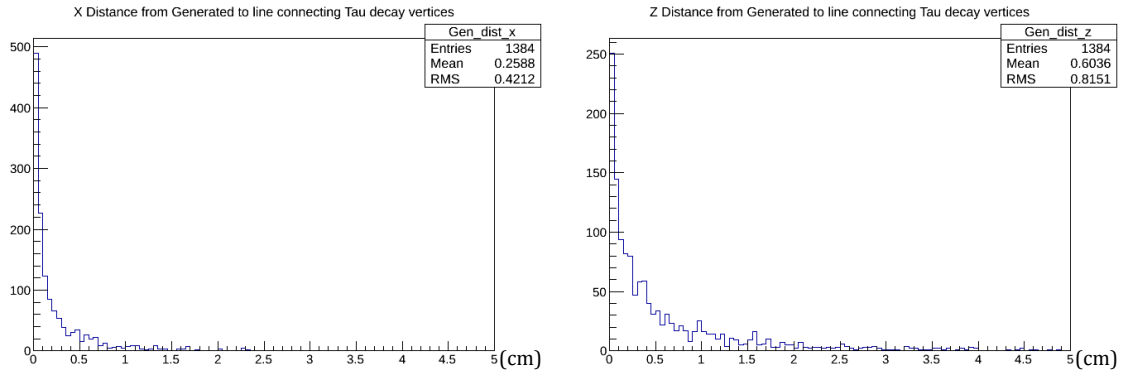


**Figure 4.2** X and Z distances from the generated primary vertex to the line connecting the tau decay vertices. The original decay model predicted the primary vertex to be on the tau trajectories, but since these distances are non-zero, this must be false. The Y distances closely resemble the plot of the X distances. The larger Z distance suggests the taus have a net momentum in the Z direction.

Although the distance in y is not shown here, it closely resembles the distance in the x direction. These plots show that the transverse distance from the primary vertex to the line is always relatively small, i.e. the x and y distances are always close to zero. However, there is a larger z distance between the primary vertex and the line. This implies that the trajectories of the tau decays are usually fairly balanced in the x and y directions, but not in z. In fact, they can both have z components of their momentum in the same direction. To get a better sense of what this actually looks like, the line connecting the tau vertices and the primary vertex were plotted for the first five events. The second event is reproduced in Fig. 4.3:

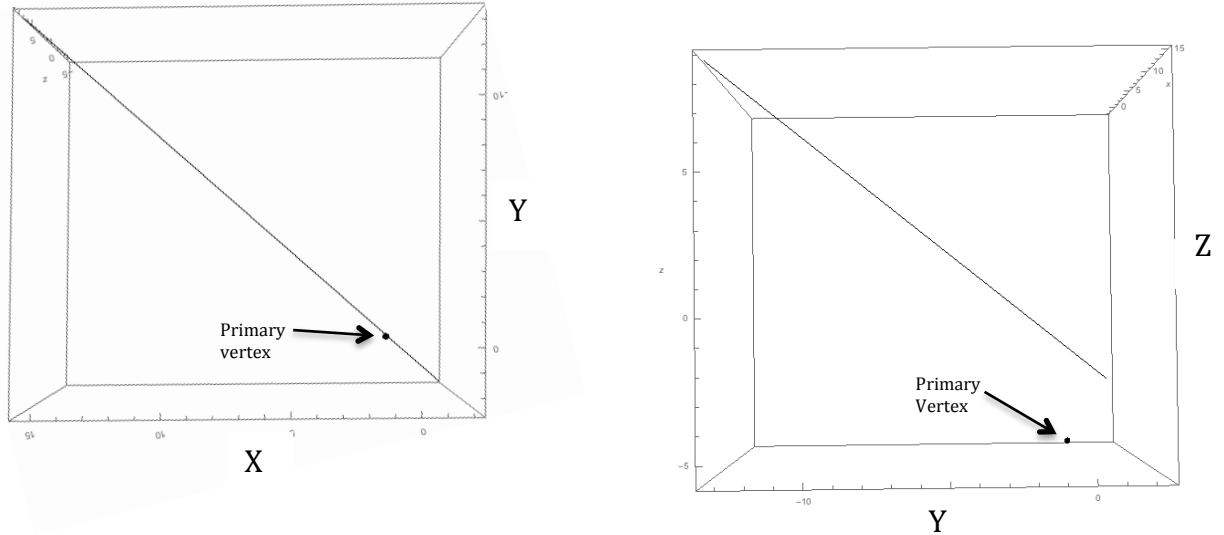


**Figure 4.3** A visual representation of one event. The plot on the left shows the primary vertex to be on the line connecting the tau vertices in the xy-plane. The plot on the right reveals that the primary vertex is actually a few centimeters below the line in the z direction.

The picture on the left shows the event in the x-y plane, with the z direction coming out of the page. It is clear that the primary vertex is essentially on the line, and any errors are small, likely a result of uncertainties in the simulation or reconstruction [4]. The picture on the right shows the same event in the y-z plane, with the x direction going into the page. Now the primary vertex is clearly not on the line, and no error can account for this discrepancy. The rest of the event plots show similar results. A clearer picture of the  $Z'$  decay is beginning to come together. By connecting the ends of the line to the primary vertex, we can see that the taus do not decay back-to-back, but appear to be boosted in the z direction.

To confirm this, plots of the combined momentum of the taus are created. The x, y and z components of these are plotted individually and compared. The results confirm a boost in the z direction:

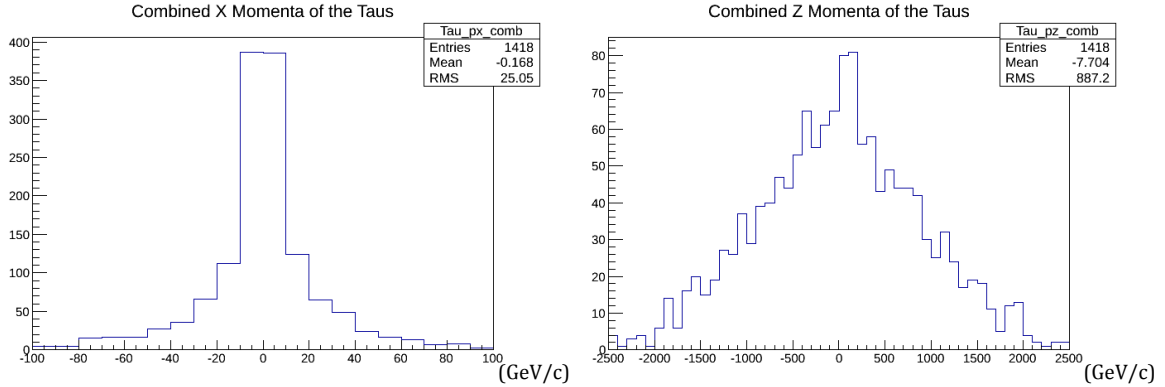
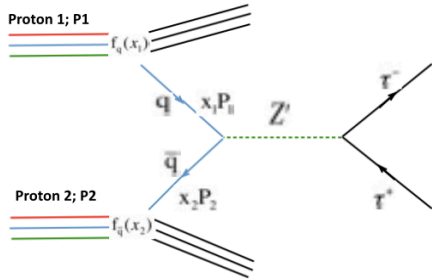


**Figure 4.4** The left plot shows that the combined X momentum is close to zero. A similar plot was made for the Y momentum, showing the same thing. The right plot shows that the Z momentum can be much larger for the taus, suggesting the  $Z'$  is boosted in this direction before decaying.

In all three cases, the combined momenta are peaked at zero, but the z momentum plot differs from the others. For the combined x momentum, i.e.  $P_{x,\tau_1} + P_{x,\tau_2}$ , approximately 60% of events have less than 20 GeV/c of combined x momentum. For the combined z momentum, the spread is much more dramatic. Almost 90% of events have more than 100 GeV/c of combined z momentum, and the tails on the histogram go all the way out to  $\pm 2500$  GeV/c. Clearly, the  $Z'$  has momentum in the z direction before it decays into the tau leptons. But why?

Initially, it was assumed that the protons accelerated around the beam pipe collided into pure energy and this was the source of the energy that created the  $Z'$ . However, the combined momentum of the protons is zero, and the momentum of the  $Z'$  is not. Therefore, it is more likely that we are dealing with a Drell-Yan process, depicted in the following diagrams:

## Leading Order of Drell-Yan



## Next to Leading Order of Drell-Yan

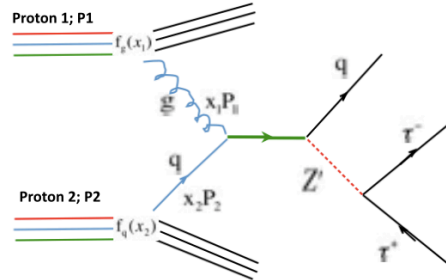


**Figure 4.5** The  $Z'$  creation is determined to be part of a Drell-Yan process, in which individual quarks/gluons within the protons interact to create the  $Z'$ . This does not change the decay of the  $Z'$ , but does allow it to have a boost.

This process is slightly more difficult to work with because it can allow the  $Z'$ , when it is created, to have a wide range of momentum values. It also means that the simple geometric picture that we started with (Fig. 4.1) is incorrect.

The algorithm that had been developed at this point cannot work with the new picture of the  $Z'$  decay, so it had to be discarded. There are no obvious ways to solve this problem geometrically, since there are a few different geometric pictures describing the same decay. Instead, correlations between the measured quantities of the electron and muon and the tau are investigated.

## 4.2 Early Fits For $P_z$ and $P_T$

In order to compare the momenta and energy of the taus to the electron and muon, each individual tau must be matched with its daughter particle. This is easily done, as they must have the same charge. The code used to create histograms was modified to match parent and daughter particles by simply comparing the signs of their charges. The equation used to calculate the mass of the di-tau system, and hence the mass of the  $Z'$ , requires the momenta of each individual tau (see background):

$$M_{Z'} = \sqrt{(E_{\tau_1} + E_{\tau_2})^2 - (\vec{P}_{\tau_1} + \vec{P}_{\tau_2})^2}$$

Since only the momenta of the electron and muon will be known when we are working with actual data from the LHC, we look for correlations between the momenta of the taus and their daughter particles.

Here, we encounter another problem. In reconstructing the simulated event, it is often the case that more than one electron or muon is identified as a candidate for an event. There are many variations when it comes to how this looks in the data. For instance, some events will have one muon and many candidates for the electron. Some will have a few candidates for both, and others will have just one candidate for each. Since there can only be one electron and one muon associated with each event, the rest must be coming from somewhere else. Many particles are created when two beams of protons collide, and their decay products fly into the detectors. The tracking software used in this process is able to track these products back to events, but it is not perfect. When two electrons, for instance, are tracked back to the same

place, the code cannot determine which one actually came from the event we are looking for, so it includes both candidates in the data. Only one of these electrons came from the  $Z'$  decay we are investigating; the other is what is called a 'fake track'. These fake tracks don't even have to be another electron. They could be something that resembles an electron, such as a charged pion, that gets caught in the electromagnetic calorimeter and is registered as an electron.

The reason that we do not simply use the generated data of the simulation, which can provide more information about an event [14], is that this information will not be available when the mass of the  $Z'$  is calculated using raw data. Though it is helpful in gaining a better understanding of the processes associated with our events, all the work associated with using reconstructed data would have to be done anyway. Overall, the simulated RECO data more closely resembles the raw data that the CMS detector will provide, so that is what is used for our analysis.

Upon inspecting the different candidates associated with any event, it is possible to visually determine which electron/muon should be used. The electrons and muons that we work with should have momentum on the order of  $10^2$  GeV/c. The  $Z'$  is created at a mass of 1500 GeV, and when this has decayed into the light electrons and muons, most of this energy has been converted into momentum. Since an individual electron makes up 1/6 of the final decay products, it is reasonable to guess it will have roughly 1/6 of the energy. This would correspond to about 250 GeV/c of momentum. The average electron momentum turns out to be 322 GeV/c. Since the  $Z'$  is boosted, it will have more than its original 1500 GeV in energy, so it makes sense that the final decay products will have a bit more than 250 GeV/c. In



most cases, when there are multiple candidates for the electron or muon, one candidate will have a reasonable momentum and the rest will have momenta on the order of 10 GeV/c or less. Thus the code used to analyze the data was modified to take the electron and muon with the highest momenta. This correctly identified the daughter particles in almost all the events. The ones for which it did not, were discarded later and will be discussed in the next section.

First, we look for direct correlations in  $P_z$  and  $P_T$ , and z direction and transverse momenta:

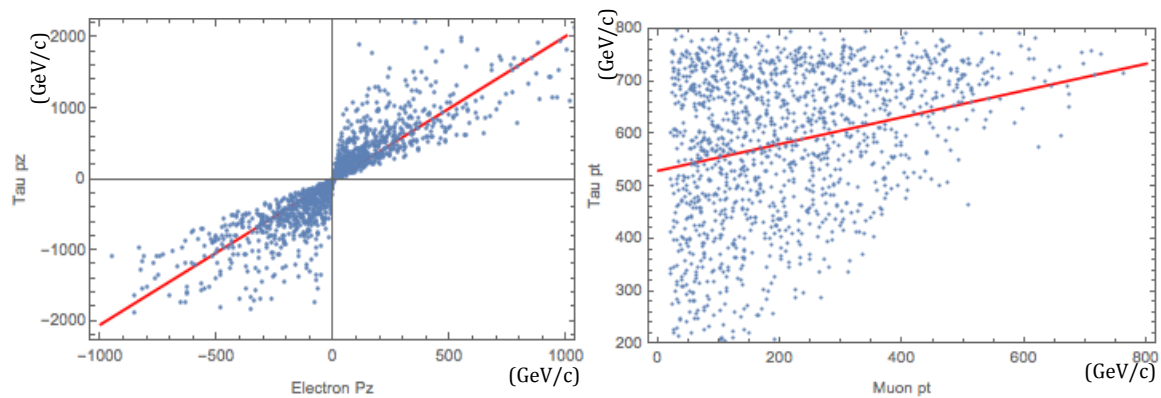


**Figure 4.6** Initial fits are done to estimate the tau momentum components. The red lines show linear plots done in Mathematica to fit the data. The left plot shows  $P_z$  of the tau vs  $P_z$  of the electron. A plot of tau  $P_z$  vs muon  $P_z$  is not included, but closely resembles the one shown here. The relationship is linear, but not strongly correlated. Similarly, the right plot shows  $P_T$  of the tau vs  $P_T$  of the muon. The plot of tau  $P_T$  vs electron  $P_T$  is not included, but closely resembles this one. There does not seem to be a correlation here.

The plot on the right of Fig. 4.6 looks poor. There does not seem to be any correlation between the transverse momentum of the tau and its daughter particle. A fit is still done, represented by the red line on the plot, but it confirms a poor linear relationship. More comparisons must be made to find a better correlation.

In the plot on the left of Fig. 4.6, there does seem to be a correlation between  $P_z$  of the tau and  $P_z$  of the electron. A very similar graph was produced for the muon and its parent tau particle. However, the fit, shown in the plot as a red line, which

has a slope of approximately 2 in both cases, looks wrong. It looks like it should be angled up more. There are a few reasons that this may be the case. With over 1,000 events, each with over a dozen pieces of data, it is impossible to check individual events for fakes. However, a few instances have been found in the data of electrons and muons with values for their momenta that exceed 2000 GeV/c. The following plot comparing the total momenta of the electron and muon shows that their individual momenta are almost always less than 1000 GeV/c.

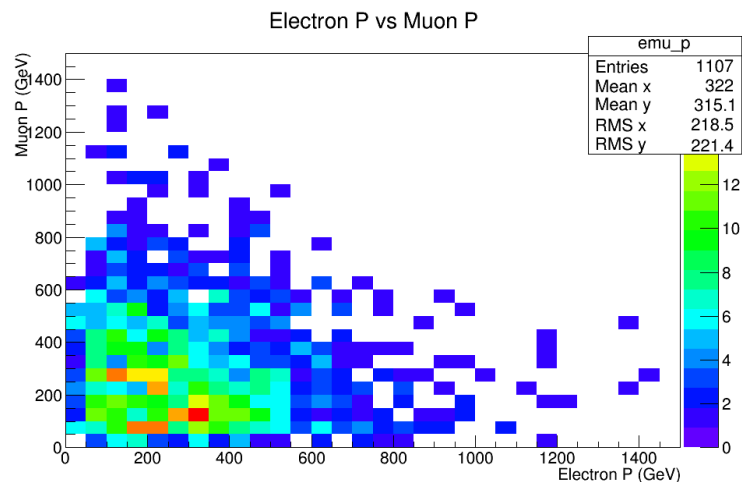


**Figure 4.7** A plot comparing the total momenta of the electron and muon. The leptons typically have less than 1000 GeV/c of momentum, so hits with much more than this are discarded as fakes.

Thus, events with electron/muon momenta exceeding 2000 GeV/c are likely due to fake tracks, and we discard them. The events that these fakes are associated with could still represent viable di-tau decays. By selecting the electron and muon hits with the highest momentum, we could be choosing the wrong ones for certain events with fakes that have too high momentum instead of too low momentum. This is a concern, but there are very few events whose selected electron/muon momenta are too high, and discarding them has an insignificant effect on the statistics of the other hundreds of events. The slope of the fit line on the plot on the left in Fig. 4.6 is

re-estimated to be approximately 3. This makes sense because the electron makes up one third of the tau particle's decay products, so it should have roughly one third of the z momentum. The same is true of the muon.

It is important to remember what these correlations and fits are meant to accomplish. Fig. 4.8 shows the plot of the generated mass of the  $Z'$ , which was calculated using the generated values of the tau momenta according to the invariant mass equation:

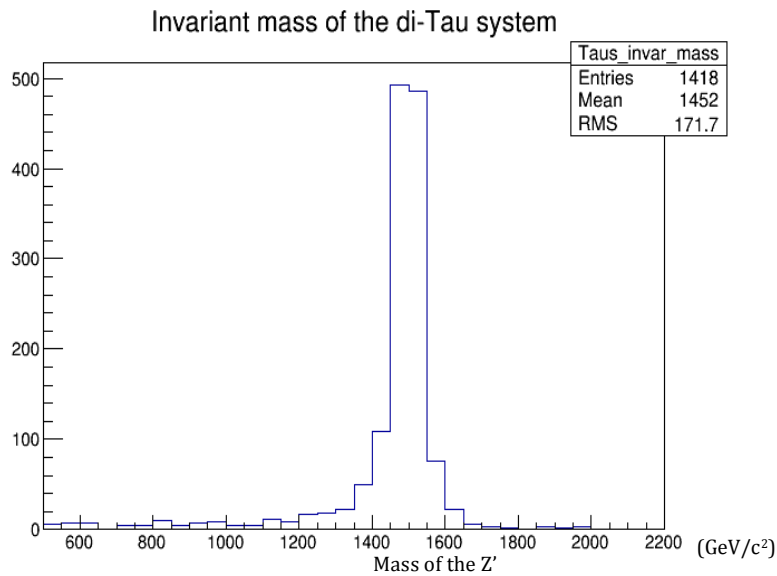


**Figure 4.8** The calculated mass of the  $Z'$  across all events.

In order to reconstruct this using only data from the electrons and muons, a method of estimating the momenta of the taus is needed. The individual momenta of the taus are needed to calculate the energy of the individual taus, and the combined momentum of the taus is needed to fill in the rest of the formula. The initial fit for the individual  $P_z$  of the taus is not very accurate. Using this in the mass equation will result in large errors. This error must be reduced in order to reproduce the

calculated invariant mass plot above. One possibility is looking for another fit in the combined  $P_z$ .

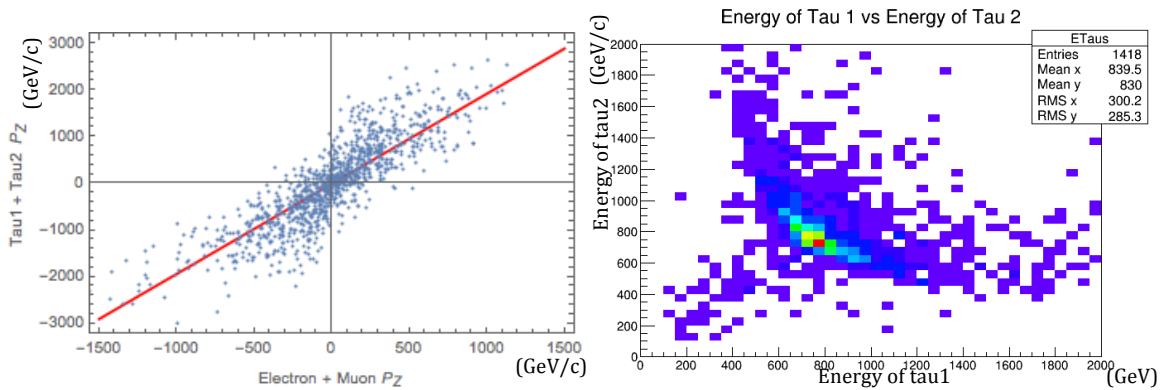


**Figure 4.9** The plot on the left shows the combined tau  $P_z$  vs. the combined  $P_z$  of the electron and muon. There is a definite linear relationship that appears to be stronger than the fit in Fig. 4.5. The plot on the right compares the energy of the taus in each event. Many taus have similar energies, but as the energy of one tau increases past  $\sim 750$  GeV, the energy of the other tends to decrease.

The plot on the left of Fig. 4.9 shows a relationship between the combined  $P_z$  of the taus and the combined  $P_z$  of the electron and muon. This is clearly a linear relationship, and appears to be better correlated than the comparison of  $P_z$  for individual taus and their daughter particles. This fit suggests that the  $P_z$  of the taus is about 2 times bigger than the  $P_z$  of the electron + muon. This fit looks better than the one done for the individual  $P_z$  values, but there is still some error. The combined  $P_z$  only appears in the mass formula once, so the error in the fit does not propagate through the mass formula as much as the fit for the individual  $P_z$  values. However, this new fit cannot be used to estimate the energy of the individual taus. The plot on the right of Fig. 4.9 compares the energy of the tau particles. The energies appear to be fairly linear for low energies up to about 750 GeV, which is the average energy of an individual tau particle. The data points below the average must come from fake tracks, because the energy of the taus has to add up to 1500 GeV, the original mass

of the  $Z'$ . Beyond that, it is likely that one tau will take away more energy than the other, but the sum of the energies typically stays below 2600 GeV. This is expected, because the combined  $P_z$  of the taus extends out to about 2500 GeV/c. For these events, almost all energy of the taus is in their z momentum, so their total energy should only be slightly bigger than 2500 GeV. Estimating the energy of the taus directly from the energy of the electron and muon is a possibility for improving our mass reconstruction formula.

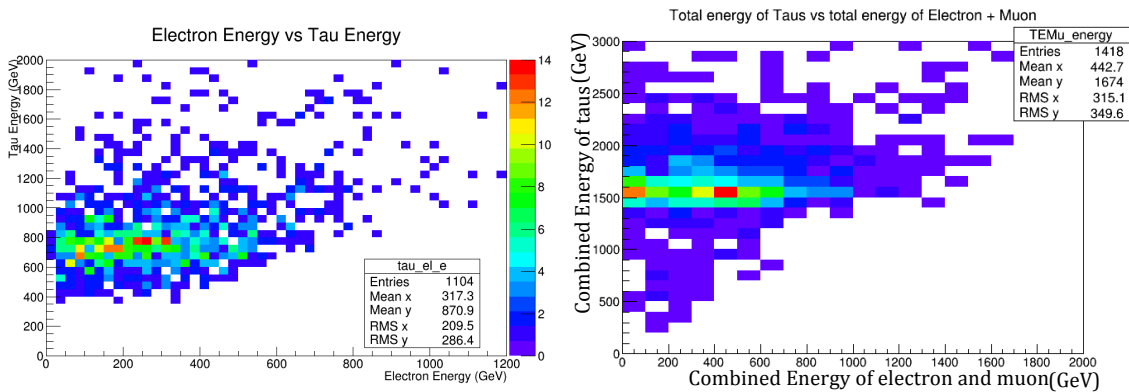


**Figure 4.10** The left plot shows the energy of a tau plotted against the energy of its daughter particle. The right plot shows the combined energy of the taus plotted against the combined energy of the electron and muon. The energy of the taus can be higher than 1500 GeV due to the  $Z'$  being boosted.

The plots in Fig 4.10 show no clear correlation between the energy of the di-tau system and the energy of the electron + muon. Since the energy is distributed among the lepton and the neutrinos in a tau decay, there is no clear implication for how much of this energy should go to the electron or muon. It is more likely to find a correlation in the momenta of the particles because there are more components involved and the direction of the momentum of the daughter particles has a dependence on the direction of the momentum of the parent particle.

We do have fits for the individual and combined  $P_z$  of the taus, each with somewhat high errors. To test the effectiveness of these fits, we estimate the mass of

the di-tau system using the fits, while keeping the generated values of the transverse momentum of the taus:

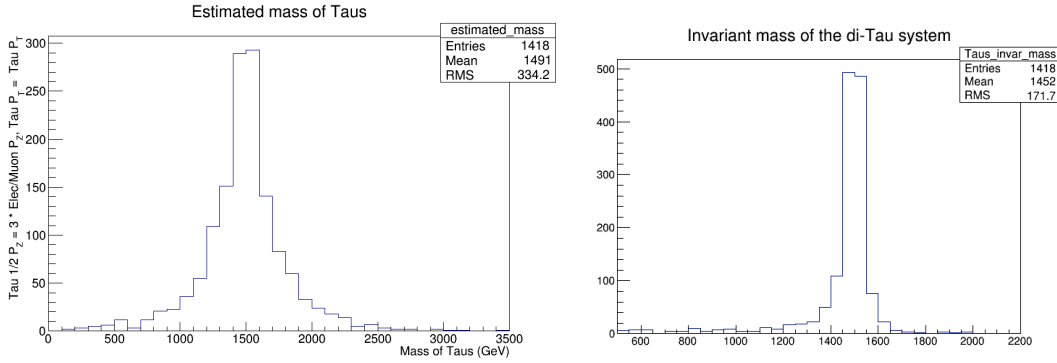


**Figure 4.11** The left plot shows the estimated mass of the system containing both tau particles. This is done using the fits for  $P_z$ . The generated values for tau  $P_T$  are used, so this method cannot be used on raw data. The plot of the actual mass of the  $Z'$  is reproduced to the right.

The plot on the left of Fig. 4.11 shows that the fit for  $P_z$  is fairly accurate, because the peak is close to 1500 GeV, but it is not as precise. The width of the peak is greater than the width of the peak on the plot of the generated mass to the right. It is a good start, but it is important to remember that such a plot could not be produced with raw data from the LHC, since this mass estimation plot uses the generated values for the transverse momentum of the taus.

The fit of the transverse momenta of the taus is too poor to be useful in reconstructing the mass. However, another idea for reconstructing the transverse momentum is to do a linear fit using both the electron and muon values, of the form:

$$P_{T,\tau} = \alpha(P_{T,e}) + \beta(P_{T,\mu}) + \gamma$$

This fit is also done in Mathematica:

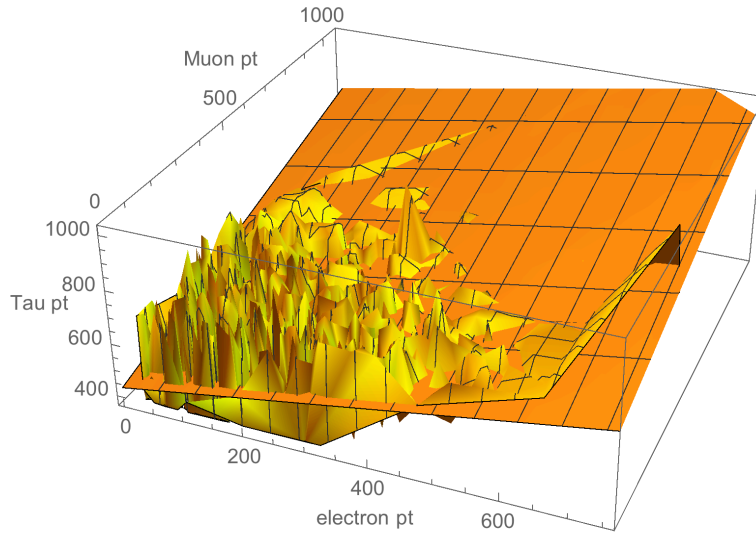


**Figure 4.12** A 3D plot fitting  $P_T$  of the taus as a linear combination of the electron and muon  $P_T$ . All values have units of GeV/c.

This fit makes a couple of assumptions. First, it assumes that the transverse momenta of the tau particles are equal. To confirm this, a plot is made comparing the transverse momenta of the taus. The second assumption states that the combined transverse momentum of the taus is zero. The need for this arises from the fact that this fit cannot estimate the combined transverse momentum of the taus, which is needed in the mass formula. Another plot is made to test the validity of this assumption. Both plots are shown in Fig. 4.13.

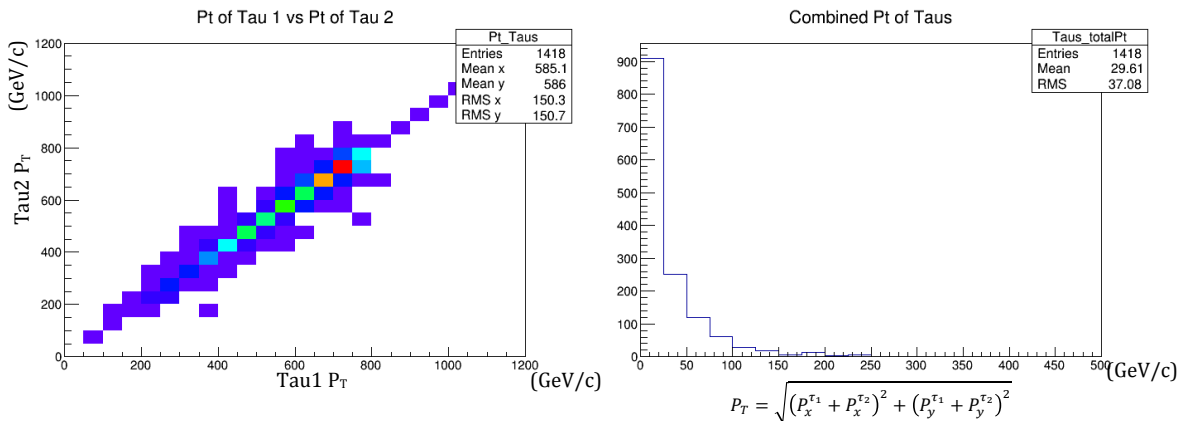


**Figure 4.13** The left plot compares the values of  $P_T$  for each tau, showing that they are always close in magnitude. The right plot shows the combined  $P_T$  of the taus. The peak at zero suggests that transverse momentum is balanced for the taus.

The plot on the left of Fig. 4.13 shows that the tau particles do, on average, have equal transverse momenta, verifying our first assumption. The plot on the right shows that the transverse momentum vectors of the taus are usually back-to-back. This is because the boost is only in the z-direction. It is possible for there to be a boost in the x or y directions because of the Drell-Yan process that creates the  $Z'$ , but this is rarely seen. The protons traveling along the beam line have all of their momentum in the z-direction, so when individual quarks or gluons within the protons interact, they are colliding with a majority of their momentum in the z-direction as well. However, it is possible for the components that make up the proton to have non-zero momentum in the x and y directions. These momenta would just be very small compared to that in the z-direction. This explains the small tail on the plot of the combined transverse momentum in Fig. 4.13.

Now that the assumptions behind our new transverse momentum fit have been verified, the fit can be tested in the same way as the previous fits. We reconstruct the mass using the fit to estimate  $P_T$  for the taus and using the generated  $P_z$  values. The result is shown in Fig. 4.14.



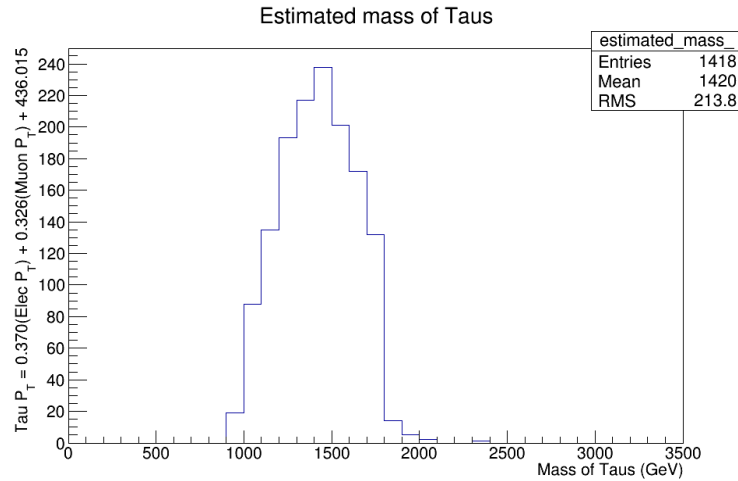


**Figure 4.14** The mass of the system containing both taus is estimated using the new fit for the transverse momentum.

Like the previous test of the  $P_z$  fit, this shows the mass of the di-tau system to be peaked close to 1500 GeV. However, it is even wider than the previous fit, so it appears to be doing a worse job of mass reconstruction in most events. Why do both of these fits manage to get close to 1500 GeV without reproducing the original mass plot? For events with a small boost, most of the momentum of the taus is transverse. In calculating the mass of these events,  $P_z$  plays a small role, and when we apply the fit for  $P_z$ , it has little effect on the mass. Thus many events can have their mass reconstructed fairly well using only  $P_T$ , as shown in Fig 4.15.

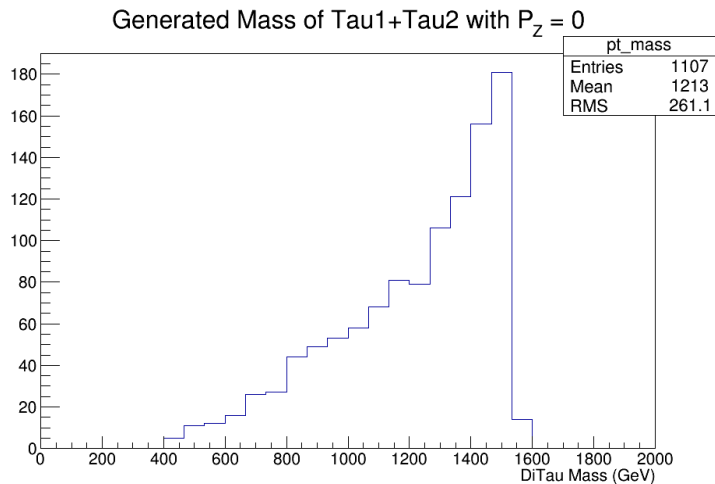


**Figure 4.15** The mass of the  $Z'$  is calculated using only the generated values for the transverse momentum of the taus. This shows that for many events,  $P_z$  is smaller than  $P_T$  and contributes less to the mass.

So even if the fits that we developed for  $P_z$  are doing a poor job, many events will still have their mass approximated well. Since all events have at least some transverse energy, using only  $P_z$  to recreate the mass does a very poor job (see A.1). From this, it is reasonable to expect the mass plot using the transverse fit to be worse just because the generated  $P_z$  values being used already account for a smaller portion of the mass in most events. This is reflected in the width of the peak on the plot for the fit of the transverse momentum, which is wider than both the plot of the generated mass and the plot for the fit of the  $z$  momentum. This suggests that the fit is not doing a good job of reconstructing the  $P_T$  of the taus. The fit for  $P_z$  appears to be doing a better job, more closely resembling the plot of the generated mass. However, it is difficult to say whether this is because the fit itself is good, or because for a large number of events, most of the energy comes from transverse momentum.

### 4.3 Comparison of Trajectory Directions

Clearly, more information is needed before an algorithm can be developed to recreate the mass of the  $Z'$ . The fact that the taus do decay back-to-back in the transverse plane raises the question of whether this might also be true for the electron and muon. Simply plotting the magnitudes against each other will not help because the two leptons can have different magnitudes of  $P_T$  and still decay back-to-back. In fact, they do have very different magnitudes in almost all events, as is seen in Fig. 4.16. Instead, the angle between the electron and muon in the  $xy$ -plane is calculated using the following formula:

$$\theta = \cos^{-1} \left( \frac{\vec{P}_{T,e} \cdot \vec{P}_{T,\mu}}{|\vec{P}_{T,e}| |\vec{P}_{T,\mu}|} \right)$$

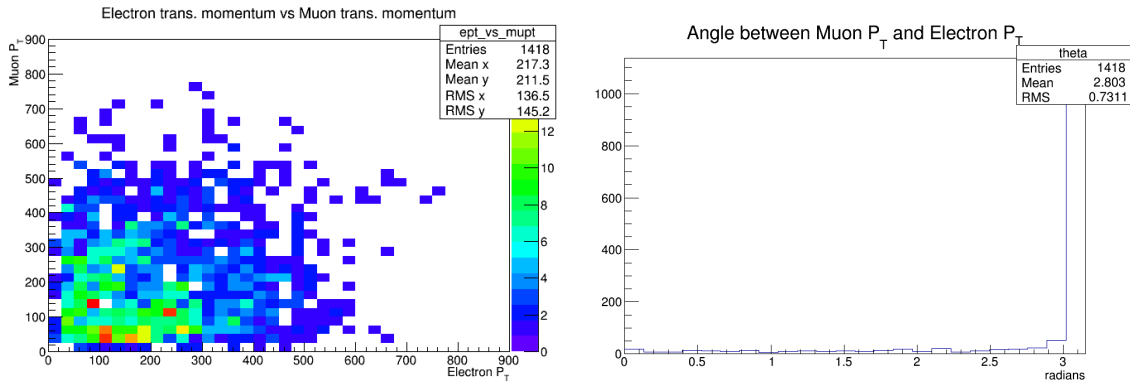


**Figure 4.16** The left plot compares  $|P_T|$  for the electron and muon. There is no correlation, but the plot on the right shows the angle that separates the electron and muon momenta in the  $xy$ -plane to be close to  $\pi$ . This suggests the electron and muon decay back-to-back in the transverse plane, just like the taus.

The plot on the right of Fig. 4.16 shows that for a majority of events, the angle between the electron and muon transverse momentum is nearly equal to  $\pi$ . The electron and muon do decay back-to-back in the transverse plane, just as the tau particles do. The generated  $Z'$  is boosted in the  $z$ -direction, but the boost in  $x$  or  $y$ , if any, is tiny. Thus, the transverse momenta of the taus, as well as what they decay

into, should be balanced. However, each tau decays into three daughter particles, and each can take some of the transverse momentum. The fact that the electron and muon are back-to-back in the xy-plane suggests that the direction of their transverse momentum is essentially the same as that of the taus from which they were created. This relationship will be explored further in the following sections.

The transverse momenta of the individual taus are not correlated to that of their daughter particles, but another variable that takes into account the direction of their respective decays could be. A likely candidate is the angle between  $P_T$  and  $P_{tot}$ , depicted in Fig. 4.17.

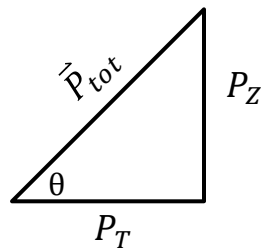


**Figure 4.17** A momentum vector can be broken into components. Here the momentum is separated into  $P_T$  and  $P_Z$ , and  $\theta$  is the angle by which the total momentum deviates from the xy-plane.

To test this, the ratio of transverse to total momentum,  $P_T/P_{tot}$ , is compared for the taus and their daughter particles. This quantity is equal to the cosine of the angle  $\theta$  in Fig. 4.17.

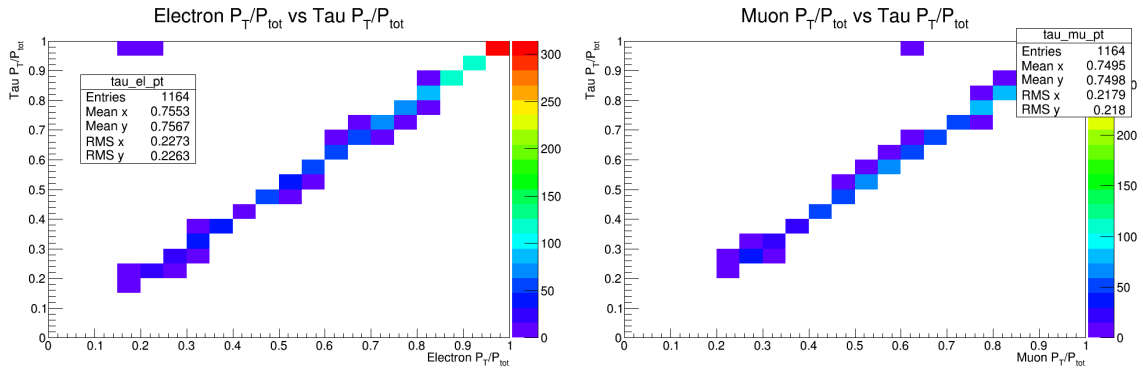


**Figure 4.18** These plots compare the ratio of transverse to total momentum for the taus and their daughter particles. In both cases, there is a very strong correlation between these quantities, suggesting the electron and muon travel in the same direction as their parent particle.

Both of the plots in Fig. 4.18 show a strong correlation between the quantities, and a Mathematica fit shows the slope to be equal to 1. So the fraction of the total momentum that is taken up by the transverse momentum is the same for the taus and their daughter particles. Since this fraction represents the cosine of the angle separating transverse and total momentum, it is likely that the angle is the same for the tau and its daughter particle. To test this, the sine of the angle, represented by  $P_z/P_{tot}$ , is compared for the taus and their daughter particles as well.

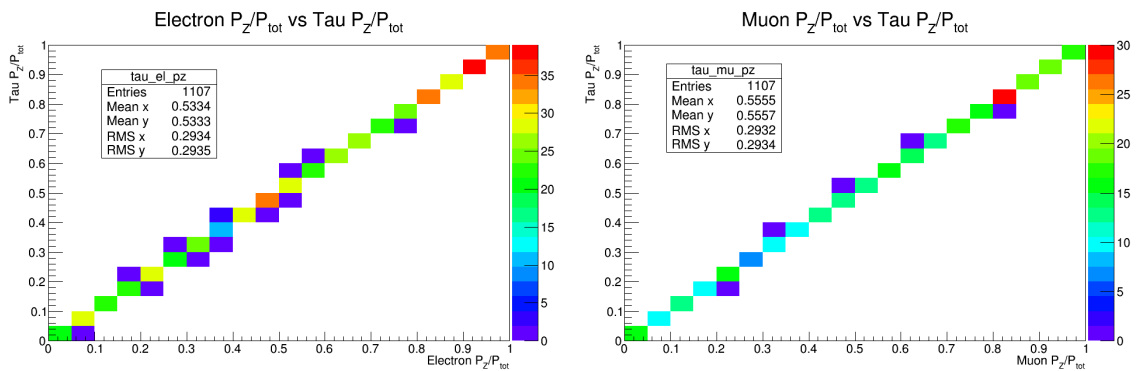


**Figure 4.19** These plots compare the ratio of the Z momentum to the total momentum for the taus and their daughter particles. This correlation, combined with the one seen in Fig. 4.17, proves that the electron and muon travel in the same direction as their parent particle.

Here, again, a strong correlation is found. The momenta of the taus and the momenta of their daughter particles point in the same direction. This can be explained by the mechanics of the tau decay. The tau has significantly more mass than the mass of the electron or muon or any of the neutrinos. Therefore, when it decays, the extra mass is converted into momentum. However, momentum must be conserved, and each daughter particle, having less mass, carries away only a fraction of the tau's momentum. Thus, the trajectories of the daughter particles are restricted into a cone centered on the tau's momentum vector, as shown in Fig. 4.20.

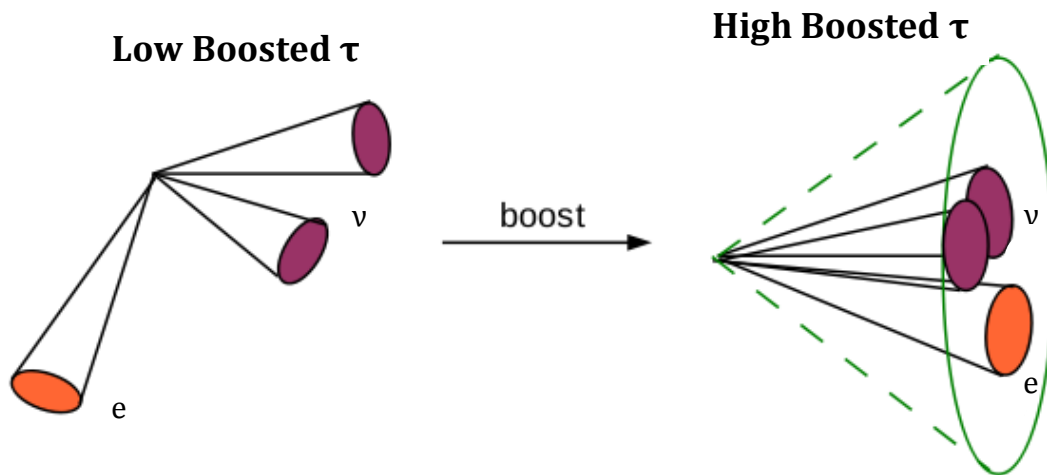


**Figure 4.20** Since the taus are highly boosted, the products of their decay are restricted into a cone centered on the tau's momentum. This explains why the electron and muon travel in the same direction as their respective parent particles after the decay [18].

The electron has a mass of  $0.511 \text{ MeV}/c^2$ ; the muon has a mass of  $105.7 \text{ MeV}/c^2$ ; the tau has a mass of  $1776 \text{ MeV}/c^2$  [19]. The masses of the neutrinos are small enough to be negligible when compared to these quantities. So the tau is over 3,000 times heavier than the electron and almost 17 times heavier than the muon. When the tau decays into one of these leptons and the two neutrinos that accompany it, their momenta are restricted to a tight cone by the high mass and

large momentum of their parent particle. This explains why the direction of the momenta are essentially the same for all events.

Now we have ways of reliably relating the transverse and z momentum of the taus to their daughter particles. However, these relations depend on the total momentum of the individual tau particles, introducing another unknown variable. A linear correlation between the total momentum of the taus and their daughter particles would be the easiest fix for this, so they are compared in Fig. 4.21:

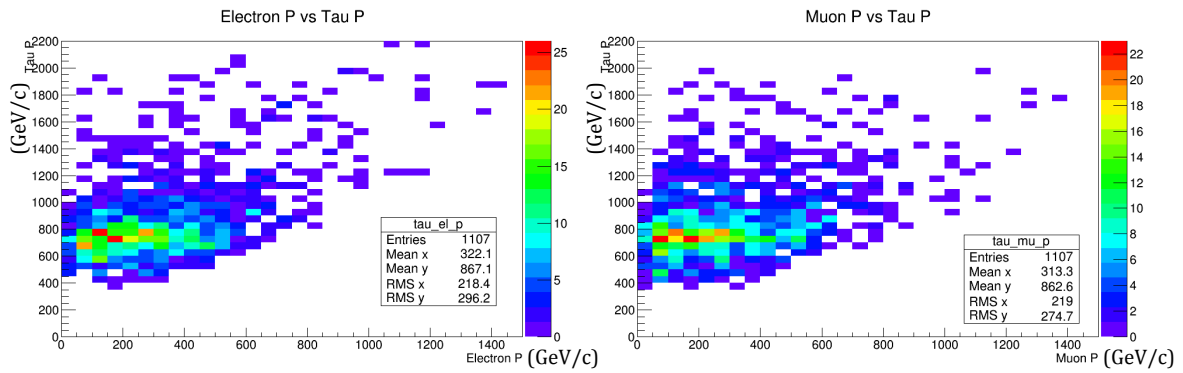


**Figure 4.21** These plots compare the total momenta of the taus to their respective daughter particles. The plots show that there are a wide range of momenta that the electron and muon can have for a given tau momentum.

These plots do not show a correlation in the total momenta. Since the total momentum can be rewritten in terms of  $P_T$  and  $P_Z$ , we technically have 6 total unknown variables. We can also use our correlations and assumptions to construct 6 equations relating the variables, so we might be able to find new correlations by manipulating them algebraically. The equations that relate the variables are:

$$\begin{aligned}
 P_{z,\tau_1} + P_{z,\tau_2} &= 2.04(P_{z,e} + P_{z,\mu}) & P_{x,\tau_1}^2 + P_{y,\tau_1}^2 &= P_{x,\tau_2}^2 + P_{y,\tau_2}^2 \\
 \frac{\sqrt{P_{x,\tau_1}^2 + P_{y,\tau_1}^2}}{\sqrt{P_{x,\tau_1}^2 + P_{y,\tau_1}^2 + P_{z,\tau_1}^2}} &= \frac{P_{T,e}}{P_{tot,e}} & \frac{\sqrt{P_{x,\tau_2}^2 + P_{y,\tau_2}^2}}{\sqrt{P_{x,\tau_2}^2 + P_{y,\tau_2}^2 + P_{z,\tau_2}^2}} &= \frac{P_{T,\mu}}{P_{tot,\mu}} \\
 \frac{P_{z,\tau_1}}{\sqrt{P_{x,\tau_1}^2 + P_{y,\tau_1}^2 + P_{z,\tau_1}^2}} &= \frac{P_{z,e}}{P_{tot,e}} & \frac{P_{z,\tau_2}}{\sqrt{P_{x,\tau_2}^2 + P_{y,\tau_2}^2 + P_{z,\tau_2}^2}} &= \frac{P_{z,\mu}}{P_{tot,\mu}}
 \end{aligned}$$

**Unknown variables are shown in red**

After manually attempting to work towards a solution to these equations, and letting Mathematica take a go at it, no solution was found. Without more information on how the momentum of the tau is related to that of its daughter particle, we cannot successfully recreate the mass of the  $Z'$ . A correlation between the momenta of the taus themselves could be useful; more plots are made comparing them, shown in Fig. 4.22:

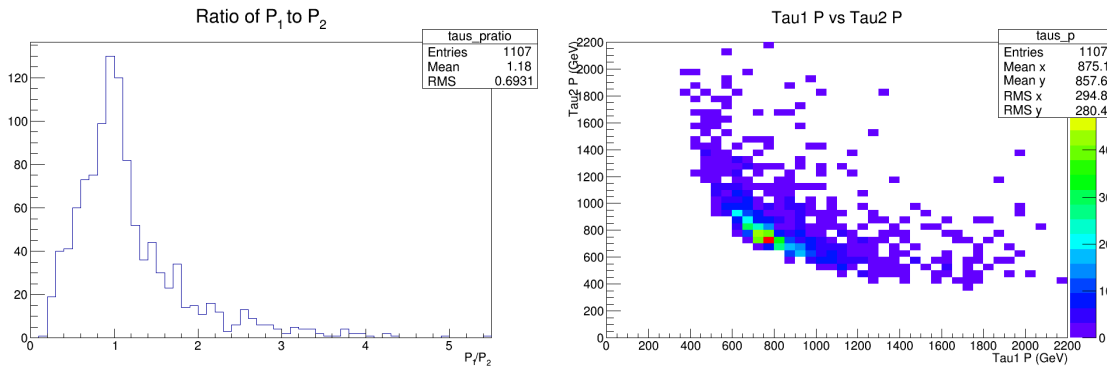


**Figure 4.22** The plot on the left shows the ratio of the taus' momenta. It varies, but is peaked at 1. The plot on the right shows the momenta plotted against each other. There is variation here as well, but it remains symmetric, as expected, since neither tau should be more likely to carry away most of the momentum.

The plot on the left of Fig. 4.22 shows that in most cases, the momenta of the taus are roughly equal, but there are also many events for which they differ significantly. The plot on the right shows that, on average, the taus share around 1700 GeV/c of momentum. It is more likely that they will share it evenly between them, but in many cases one tau carries away significantly more momentum than the other. This information does not immediately suggest a way to solve for the momenta of the individual taus. Since we still do not have a way of relating the momenta of the taus to anything, we cannot determine their individual components.



#### 4.4 Missing Energy

In the background, missing energy is described as a way of identifying ‘invisible’ neutrinos. It can be represented as a neutrino carrying away the momentum needed to balance a decay. In the case of a single neutrino in the decay products, this missing energy is relatively straightforward to calculate. Since the momentum should be balanced in the transverse plane, the momentum of the neutrino just points in the opposite direction of the sum of the momenta of the other products. Thus, all the momenta add to zero. In our case, we have two neutrinos for each tau decay, so the best we can do is perform the calculation as if there is only one. If all the masses and momenta of the decay products were known, the mass of the  $Z'$  could be calculated by just solving for the invariant mass of the system containing all its decay products. Fig. 4.23 shows this being done with and without the missing energy.

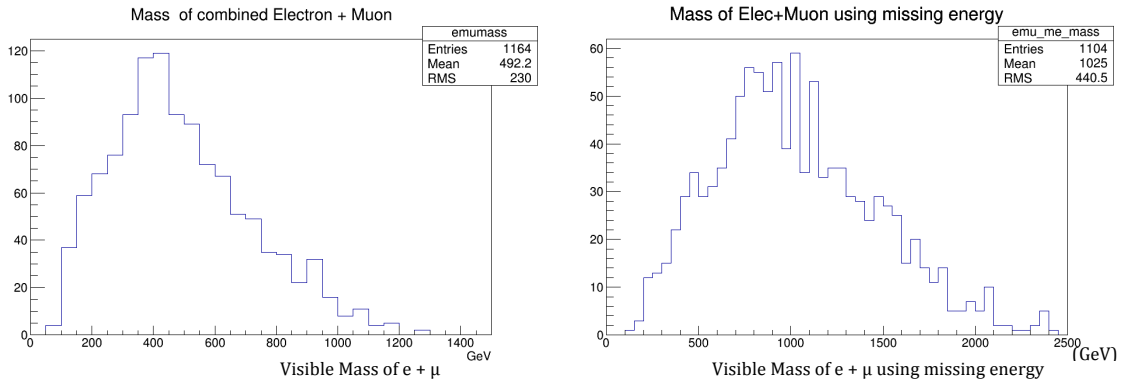


**Figure 4.23** The left plot shows the mass of the system containing the electron and muon. The right plot shows the same thing calculated with the addition of the event’s missing energy, where the missing energy was calculated individually for both tau decays, i.e.  $E_{T,e} = -P_{T,e}$  and  $E_{T,\mu} = -P_{T,\mu}$ .

It is clear that neither of these plots does a good job of actually recreating the mass of the  $Z'$ . The plot on the left shows that the combined mass of the electron and muon is peaked at 400-450 GeV. These particles make up a third of the decay

products, so it is not surprising that their mass usually accounts for about a third of the original 1500 GeV that the  $Z'$  had. However, the large spread in this graph means that we cannot simply shift the plot up by 1000 GeV. By including the missing energy of the system, the mass is shifted up, but the spread is worse. The mass is still underestimated because we cannot account for all the extra energy of the four neutrinos. If a better estimate of the missing energy was possible, it could improve this method.

Another helpful aspect of incorporating missing energy relates to the reduction of background signals. Recall that once an algorithm is developed to reconstruct the mass of the  $Z'$ , this algorithm has to be tested against background signals that mimic the di-tau decay we are investigating. Most of the methods of mass reconstruction discussed thus far could also work on another decay, such as the  $W^+W^-$  decay (See Background). This decay also produces an electron and a muon, but in this case, the  $W$  bosons are either created at the beam spot in the proton-proton collision, or a particle that was produced by the collision, such as the Higgs boson, will decay into  $W^+W^-$  [3]. This process can pass many of the selection cuts described in the background because the Higgs has a high mass compared to the electron and muon. To avoid registering such false hits, we look for other variables that can distinguish such events. A good place to start, it turns out, is with missing energy. When the missing energy of the  $Z'$  system is plotted against the difference in  $P_T$  between the electron and muon, there is a fairly strong one-to-one ratio. This can be seen in the left plot of Fig. 4.24. When the same thing is done for the  $W^+W^-$  background signal, there is not such a strong correlation, as shown in the

plot on the right of Fig. 4.24. Therefore, by using the difference in  $P_T$  instead of the missing energy, we can reduce some of the background signals.

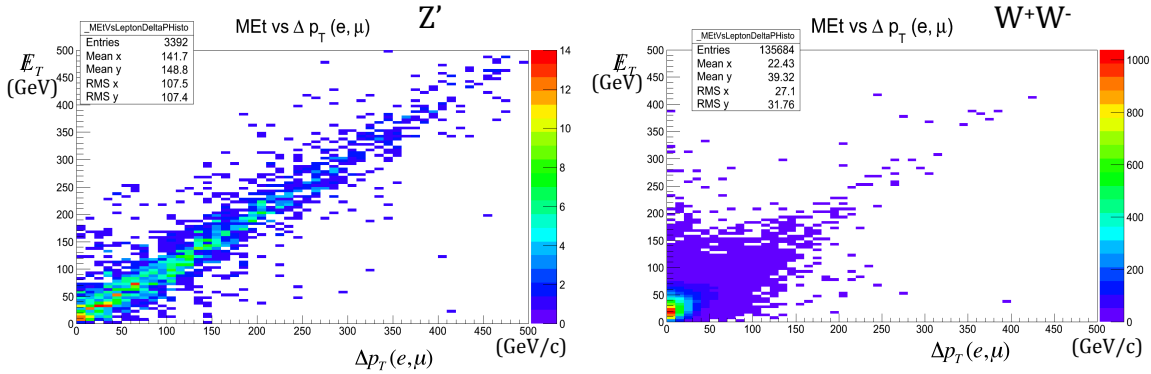


**Figure 4.24** Plots are made comparing the missing energy associated with an event to the difference in transverse momentum between the electron and muon. For the  $Z'$  decay that we are looking at, there is a strong linear relationship here. For background signals, such as  $W^+W^-$ , there is not such a strong correlation. This information can help reduce backgrounds.

The reason for this likely has to do with the way the  $W^+W^-$  channel is produced. It is often accompanied by jets (see Background) which also account for a portion of the energy. Since this energy is not considered when calculating the missing energy, but it still affects the final energies and momenta of the electron and muon, the linear relationship is skewed for decays that involve one or more jets.

This method also works to distinguish the  $Z'$  decay from the  $t\bar{t}$  decay (see Background). This decay involves b jets that carry away lots of energy, making the missing energy even more difficult to calculate. Another plot of  $\Delta P_T$  against the missing energy for the  $t\bar{t}$  system is shown in Fig. 4.25:

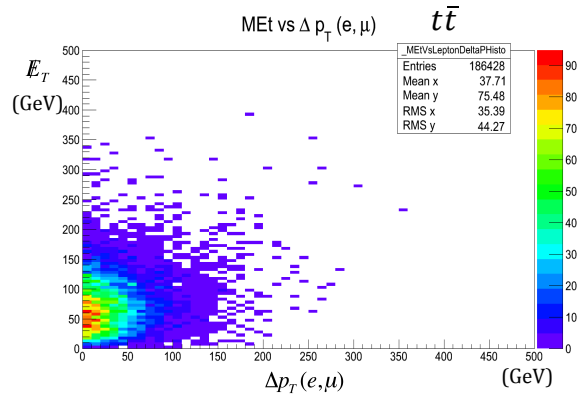


**Figure 4.25** Plot comparing the missing energy calculated for  $t\bar{t}$  events to the difference in transverse momenta between the electron and muon. The lack of a linear relationship helps distinguish this event from the  $Z'$  decay we are investigating as well.

Here the correlation is even less linear than in the  $W^+W^-$  decay because there are more jets associated with  $t\bar{t}$  decays. This shows that these common background signals can be separated from the  $Z' \rightarrow \tau^+\tau^-$  signal that we are looking for. Therefore, future mass reconstruction methods should use  $\Delta P_T$  in place of any missing energy terms as a means of reducing background signals.

## 5. Results

By using the individual fits for  $P_Z$  of the taus, we can estimate the total momentum of each tau with the following formula:

$$|\vec{P}_\tau| = 3 \times |\vec{P}_l|,$$

where  $|\vec{P}_l|$  is the magnitude of the total momentum of the lepton that the tau decays into, i.e. the electron or muon. This can then be used to estimate the transverse momentum of the tau with our other relation,

$$P_{T,\tau} = |\vec{P}_\tau| \times \frac{P_{T,l}}{|\vec{P}_l|}$$

Now a rough estimate of the mass of the  $Z'$  can be produced with the familiar mass equation.

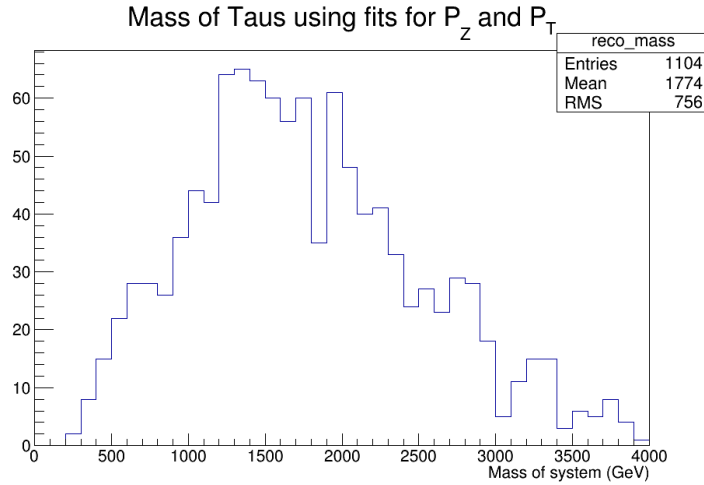


**Figure 5.1**  $Z'$  mass calculated using  $P_{Z,\tau} = 3 \times P_{Z,e/\mu}$  and  $P_{T,\tau} = |\vec{P}_\tau| \times \frac{P_{T,e/\mu}}{|\vec{P}_{e/\mu}|}$

This can be compared to the mass plot created by calculating the mass of the electron and muon, including the missing energy of the event.

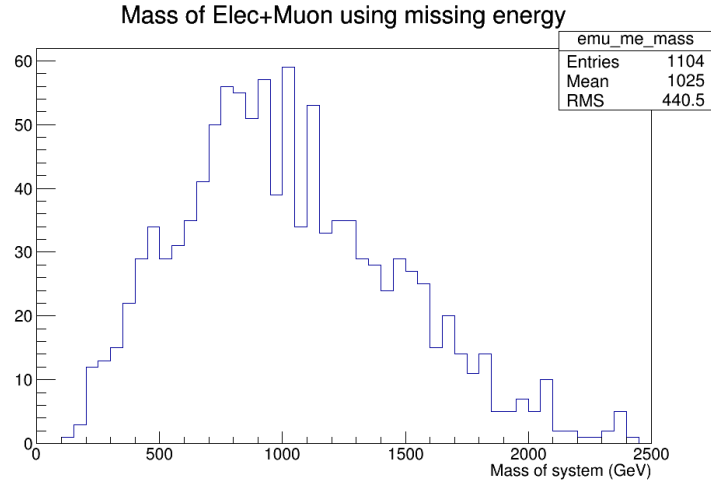


**Figure 5.2** Mass of the combined electron and muon, using missing energy calculated for the electron and muon individually, i.e.  $\vec{E}_{T,e} = -\vec{P}_{T,e}$  and  $\vec{E}_{T,\mu} = -\vec{P}_{T,\mu}$

Neither of these methods does a great job of reconstructing the original mass, which peaks much more sharply at 1500 GeV/c<sup>2</sup>.

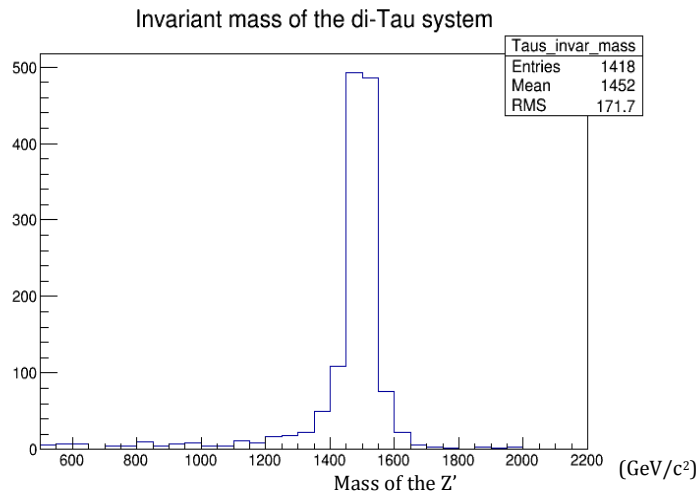


**Figure 5.3** Generated mass of the Z'.

As of now, these are the only means we have of estimating the mass of the Z' directly from the electron and muon momenta. Using the missing energy, we can differentiate between the Z' decay process and some of its background signals, which is the next step in the project. However, an accurate mass reconstruction is still needed.

## 6. Discussion

In this project, we tried to find a way to solve for the variables in the formula for the invariant mass of the system containing the tau particles. We found a correlation in  $P_z$  between the taus and their daughter particles. When compared individually, the tau has about 3 times as much  $z$  momentum as its daughter particle. When this fit was done for the electrons and their parent tau particles, the standard deviation was calculated by applying a sum of squares over all events. The standard deviation came out to be 290 GeV/c. The same was done for the muons and their parent taus, and the standard deviation came out to be 320 GeV/c. Another fit was done to compare the combined  $z$  momentum of the taus to that of the electron and muon. This fit suggested that the  $P_z$  of the taus is 2.04 times bigger than the  $P_z$  of the electron and muon. The calculated standard deviation for this fit is 480 GeV/c, which is less than the sum of the standard deviations for the previous two fits. This shows that it is better to estimate the sum of the tau  $P_z$ s than to add the individual estimates.

The standard deviations for the  $P_z$  fits are high. There is certainly a linear relationship here, but it is not that strong. Most points fall around 300 GeV/c from the line describing the fit. An error this large causes problems when calculating the mass of the di-tau system. It is the reason that the plot of the mass incorporating these fits is so broad. If we drop the points that lay more than one deviation from the line, then we lose a lot of events that contain the decay we are looking for, and if we do this for all three fits then we lose more than half of our data points. These are drastic measures just to get a fit that describes the data well. Such a fit would not be

helpful when we incorporate raw data, which are expected to vary as much as our simulated data.

The fits done for direct comparisons of the transverse momenta were poor, and it was obvious that they could not be used to recreate the mass. Still, they did lead to some insights about other properties, such as the back-to-back decay of the electron and muon in the transverse plane, that were helpful.

The most significant correlations found were for  $P_T/P_{\text{tot}}$  and  $P_Z/P_{\text{tot}}$  between the taus and their daughter particles. These were almost perfectly 1:1. The standard deviations of these four fits are all  $\sim 0.001$ , showing how exact the correlation is. The taus do have the same angle associated with their trajectory as their daughter particles. When the boosted tau particle decays, the cone representing the allowed trajectories of its products is so narrow that the angles only differ by about one part in a thousand.

The problem with relating two known quantities with two unknown quantities is that more information is needed to solve for each variable. So just knowing  $P_T$  and  $P_Z$  for the electron is enough to determine the ratio of  $P_T$  to  $P_Z$  for the tau, but it is not enough to solve for either of these variables. At this point we have six variables needed to calculate the mass of the  $Z'$ , and six equations to relate them. If these equations were linear, and a solution existed, we would be able to solve for it. However, five of these equations contain quadratics, so even if a solution exists, it is possible that these equations are not enough to find it. Indeed, attempts to simultaneously solve these equations have not been successful. No information



suggests a trend that can be written as an equation to assist in this yet. It is unclear where to even look for such a trend.

Reconstructing the mass from the components of the electron and muon momenta and missing energy did not get close to the plot of the generated  $Z'$  mass either. However, investigating this missing energy and its relation to  $\Delta P_T$  of the electron and muon did yield a way of distinguishing the  $Z' \rightarrow \tau^+ \tau^-$  decay from some of its background signals. This suggests that if  $\Delta P_T$  can be directly used to calculate the mass of the  $Z'$ , our algorithm will already cut out many background signals. If it cannot be used directly, this information can still be used to reduce background signals separately. There is no obvious way to use  $\Delta P_T$  to help reconstruct the mass, but this is another possible route to explore.

## 7. Conclusion

After inspection of the electron/muon channel in the di-tau decay, no algorithm was found that was capable of accurately reconstructing the mass of the  $Z'$ . Our initial geometric approach was developed under the assumption that the  $Z'$  is not boosted. This notion was soon debunked by comparing the distances and directions that the tau particles travel before they decay. The events in the datasets we worked with displayed a range of boosts in the positive and negative  $z$ -directions, with a spike close to zero GeV/c. This hinders a geometric approach because many different pictures of the decay can be drawn and a method that works on one may not work for another diagram.

The geometric approach was abandoned and instead reconstructing the mass was attempted using the momenta of the electron and muon. The fits found for  $P_z$  and  $P_T$  were not able to reproduce the generated  $Z'$  mass, and the discovery that the electron and muon travel in the same direction as their parent tau particles did not yield enough information to improve these fits.

There is a chance that there is a correlation between how far off from one of these fits a data point is and some other variable. If this was true, then an algorithm could possibly be developed that treats individual events differently depending on some characteristic of the electron and/or muon. Plots were made to compare the mass of the system containing the electron and muon to a few different variables (see A.2). No patterns were found, but there are many other comparisons that can be made. It is impossible to say whether such a correlation exists, and if one does, it is impossible to say whether an algorithm could incorporate it. There was not

enough time during this project to explore this possibility, but future experiments should be mindful of it.

Another possibility would be to incorporate decay lifetimes to help reconstruct the  $Z'$  mass. This would have been used as the final step in the geometric algorithm, since the distance the tau particles travel before decaying can be used to calculate their boost. It is unclear as of now how lifetimes can be used in the mass reconstruction of the  $Z'$ , but its potential for estimating the energy of the taus should not be ignored.

Finally, it may be the case that there is no good way to reconstruct the mass of the  $Z'$  using the electron/muon channel. The four neutrinos carry away a lot of important information about the system, and the boost of the  $Z'$  distorts what could otherwise be a solvable geometric problem. If no reasonable algorithm can be developed, we may have to pursue other channels. The rest of the channels associated with the tau decay hadronically. These channels produce one or more jets of hadrons inside the detector. Since hadrons are produced in many decay processes, and they tend to produce a lot of daughter particles, tracking jets is challenging. These jets can also produce their own missing energy, often including neutrinos. For these reasons, the electron/muon channel was investigated first. However, work has been done elsewhere to provide better analysis of hadronically decaying taus [8]. Focusing on the hadronic channels would mean losing the opportunity to increase overall understanding of the electron and muon channels, but it may prove necessary if none of the other proposed pursuits is successful.

## 8. References

- [1] P. Langacker, “The Physics of Heavy Z-prime Gauge Bosons”, *Rev. Mod. Phys* **81** (2009), doi: 10.1103/RevModPhys81.1199
- [2] T. Rizzo, “Zprime Phenomenology and the LHC”, *Published in Boulder, 2006, Colliders and Neutrinos (TASI 2006)* [arXiv:hep-ph/0610104] (2006).
- [3] CMS Collaboration, “Search for neutral Higgs bosons decaying to tau pairs in pp collisions at  $\sqrt{s} = 7$  TeV”, *Physics Letters B*, Volume 713, Issue 2, 21 June 2012, Pages 68-90, ISSN 0370-2693, <http://dx.doi.org/10.1016/j.physletb.2012.05.028>.
- [4] The EXO Tau Group, “Search for High Mass Resonances Decaying to Taus with  $\sqrt{s} = 8$  TeV”. CMS AN-12-309 (2013).
- [5] J. Stanislaw, et al, “TAUOLA- A Library of Monte Carlo Programs to Simulate Decays of Polarized  $\tau$  Leptons”, CERN-TH-5856/90 (1990).
- [6] J. Beringer et al. (Particle Data Group), “ $\tau$  Branching Fractions”, *PR* **D86**, 010001 (2012), <http://pdg.lbl.gov>.
- [7] P. Burchat, “Decays of the Tau Lepton”, Stanford University, 1986. <http://www.slac.stanford.edu/pubs/slacreports/reports14/slac-r-292.pdf>
- [8] D. Buskulic, D. Casper, I. De Bonis, D. Decamp, P. Ghez, et al., “Tau hadronic branching ratios”. *Zeitschrift für Physik C Particles and Fields*, Springer Verlag (Germany), 1996, 70, pp.579-608. <in2p3-00001563>
- [9] <http://physics.info/standard/>
- [10] Griffiths, David. “Introduction to Elementary Particles”. Second. Germany: WILEY-VCH, 2008.
- [11] A. Pich, “Precision Tau Physics,” Department de Física Teòrica, IFIC, Universitat de València, *Prog.Part.Nucl.Phys.* 75, pp. 41-85 (2014).
- [12] CMS detector citation: CMS Collaboration, “The CMS experiment at the CERN LHC”, *JINST* **3** (2008) S08004, doi: 10.1088/1748-0221/3/08/S08004.
- [13] <http://cms.web.cern.ch/>
- [14] <https://twiki.cern.ch/twiki/bin/view/CMSPublic/WebHome>
- [15] <http://geant4.cern.ch/>
- [16] <https://inspirehep.net/record/1121128/plots>
- [17] [https://esc.fnwi.uva.nl/thesis/apart/phys/thesis\\_nl.php?level=master&start=101](https://esc.fnwi.uva.nl/thesis/apart/phys/thesis_nl.php?level=master&start=101)
- [18] <http://www.quantumdiaries.org/2012/08/05/boost>
- [19] K.A. Olive et al. (Particle Data Group), *Chin. Phys. C*, **38**, 090001 (2014).

## 9. Appendix

### A.1 $P_z$ Mass

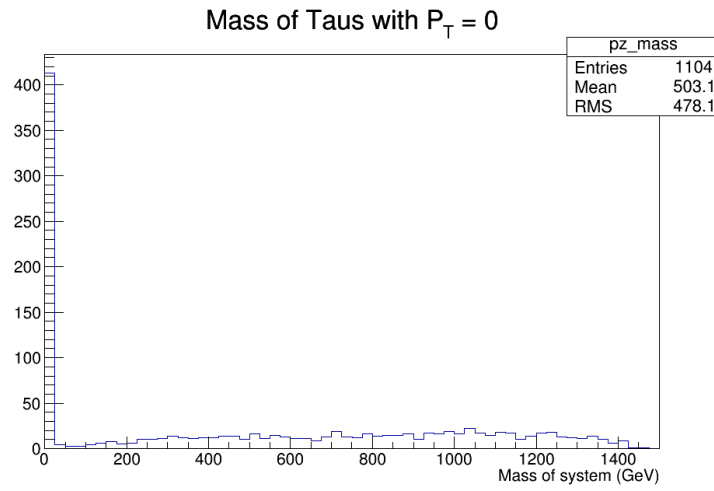


**Figure 9.1** The generated mass of the taus, calculated using only the mass and  $P_z$  of the taus. For almost all events, this does a terrible job of reconstructing the mass. Clearly,  $P_z$  does not play as big of a role in the mass formula as  $P_T$  (see 4.2).

## A.2 Comparing the Mass of $e + \mu$ to Various Quantities

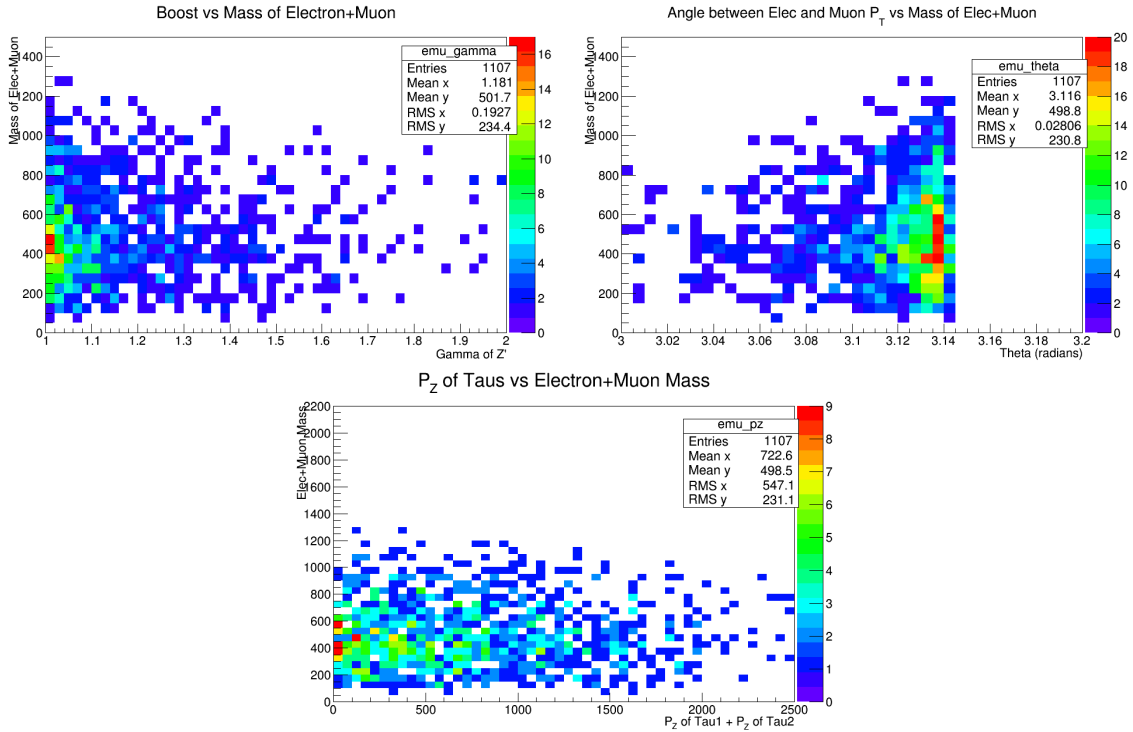


**Figure 9.2** Plots are made comparing the combined mass of the electron and muon to three quantities. In the upper left plot, it is compared to the gamma value associated with the boosted tau, calculated as  $\gamma = \frac{E}{m}$ , where  $E$  is the combined energy of the taus, and  $m$  is  $1500 \text{ GeV}/c^2$ . In the upper right plot, the  $e\mu$  mass is compared to the angle separating the electron and muon transverse momentum vectors. The bottom plot compares the mass to the combined  $z$  momentum of the taus. None of these plots shows a correlation that can be used to reconstruct the mass of the  $Z'$ , but there are many more variations that can be tested.